Universiteit Utrecht

# BioSealing A Single Hole Fractured Rock

MSc Water Science & Management Thesis

Abi Satria Praga
Student Number: 5766354
abisatriapraga@students.uu.nl
May 17, 2021

1st Supervisor: Prof. dr. R.J. Schotting
R.J.Schotting@uu.nl
Chair of the Environmental - Hydrogeology Group
Department of Earth Science
Faculty of Geoscience
Utrecht University

2nd Supervisor: dr. A. Raoof
A.Raoof@uu.nl
Assistant Professor
Department of Earth Science
Faculty of Geoscience
Utrecht University

Thesis Coordinator: dr. P. Schott
P.P.Schot@uu.nl
Associate Professor
Copernicus Institute of-Sustainable Development
Faculty of Geosciences
Utrecht University

# Abstract

Climate change poses a threat to freshwater availability around the world, especially in dryland regions. Yunnan province of China is one such region that is facing this problem. Even though Yunnan rains just as much as the Netherlands, a country considered to be 'wet', the province is experiencing a shortage of groundwater which contributes to its degraded land and lack of water supply for its population. It follows that climate change is not the only factor contributing to the shortage of groundwater. The bedrock in the subsurface is fractured, allowing for rapid infiltration of water to seep towards deeper depths, which is why little to no groundwater is found beneath the soil surface.

To solve this issue, a cheap and environmentally friendly solution that can seal these subsurface fractures is needed to establish a groundwater table in the overlying soil. BioSealing, a proven technique developed by Deltares using nutrients to feed naturally occurring microorganisms in the soil to grow biomass to seal leaks, could be that solution. This leads to the research question of this study, which is "To what extent is the BioSealing technique effective in sealing a single hole fractured rock to establish a groundwater table in the overlying soil?".

To address the question, a sandbox type experiment with the BioSealing technique was conducted from a top-down approach under unsaturated conditions to seal a single hole plate that mimics a fractured bedrock. To observe the effectiveness of BioSealing, the decline in effluent flow rate was monitored and analyzed for its clogging factor. The saturation distribution was also measured for a potential rise in groundwater table by using the dual gamma-ray transmission method and 5TE sensors. To ensure that BioSealing took place in the correct area of the soil system, a bacterial count analysis was done per layer.

The experiment results were hindered by an unexpected outcome of a saturated tank, even though nutrients were not injected yet. This meant that establishing a groundwater table is no longer possible, so a decision was made to continue the experiment under saturated conditions. Despite the tank being fully saturated, the saturation measurements fluctuated for every measured location after some nutrients were present in the soil, indicating that BioSealing has taken place. The effluent flow rate declined with a clogging factor of 11 as a result. However, the extent to which this was due to BioSealing near the surrounding area of the leakage hole is doubtful because the bacterial count analysis revealed that most of it occurred just below the soil surface and only some happened near the leak.

As a consequence of the results, this research cannot fully address the research question but can conclude, to a small extent, that BioSealing is effective in reducing the seepage flow rate. Some knowledge and insights found in this study validated some theories and experimental results from BioSealing and bioclogging literature as well.

# Contents

# List of Figures

# List of Tables

# 1. Introduction

## 1.1. Freshwater Stress: From Climate Change to Fractured Rock

The availability of freshwater in the world is constantly under threat due to human and natural causes (Kummu et al., 2016). This issue is further exacerbated by climate change as it induces changes in meteorological factors such as precipitation and temperature, which has led to an increase in the frequency of extreme events like droughts (Mukherjee, Mishra, & Trenberth, 2018). Dryland regions of the world are the most vulnerable to droughts and consequently water stress, even when global temperatures are under 2 °C – which is a target of the Paris Agreement (Huang, Yu, Dai, Wei, & Kang, 2017). Droughts negatively impact various sectors and systems that depend on water resources such as forests, agriculture, transportation, human health, energy, water supply, and sanitation (Kundzewicz et al., 2008). For example, in the agricultural sector of Mozambique, a median temperature increase of 2-4 °C and variable changes in precipitation by 2100 can cause a -8% to -16% yield for wheat crops (Adhikari, Nejadhashemi, & Woznicki, 2015). In India, a temperature increase of 1-3 °C can lead to a yield reduction from 10% to 72% for all crops (Chauhan et al., 2014). Similar drought impacts can also be seen in the Yunnan province of China (Qiu, 2010).

Qiu (2010) noted that the Yunnan province received 60% less rainfall than normal and experienced more frequent droughts. As a result, 18% of their population (8.1 million people) were short of drinking water, and it was expected that US$2.5 billion worth of crops failed. Interestingly, despite receiving 60% less rainfall, the average annual precipitation of Yunnan is at least 1000 mm, which is more than what the Netherlands is receiving (800mm per year) – yet the Netherlands is considered a 'wet' country (Schotting, n.d.). Climate change does play a role in making Yunnan a dry land as they saw a decrease in rainy days and increase in droughts and short torrential rains since the 1960s; however, it is not the only reason causing the land to be very dry (Qiu, 2010).

Deforestation for human uses like settlements and agriculture (land-use change) also contributed to drought impacts (Qiu, 2010). The natural forests of Yunnan used to provide strength, structure, organic matter, and moisture in its soil for vegetation to develop so that it can regulate climate and hydrological processes. With the forests nearly gone, Yunnan experienced more land degradation, landslides, and flash floods. In addition to deforestation, it does not help that some areas of Yunnan are situated on top of fractured limestone rock, causing rapid infiltration of rainfall (Andersen, 2013). It is believed that these fractures in the rock layer explain why there is hardly any groundwater table in Yunnan's topsoil – further contributing to land degradation (Schotting, n.d.).

Furthermore, the rainwater stored in the fractures and the underlying aquifer can be as deep as 150 m below ground level. Tapping into this groundwater resource by drilling into these depths is not feasible due to the deplorable economic conditions of Yunnan. Other dryland regions in the world are in a similar situation as Yunnan, and solutions are needed to help them.

## 1.2. BioSealing as a Potential Solution?

Potential solutions to help solve freshwater stress and its secondary effects like land degradation, especially in dryland regions such as Yunnan, can be simplified to two strategies: (1) increase water supply and (2) reduce water loss. One of the best and affordable ways to increase water supply is to harvest rainwater, where rainwater is collected and stored during wet periods and can be used later during dry periods (Helmreich & Horn, 2009). This can be implemented for various uses; however, rainwater harvesting techniques are limited in their storage capacity size – which may not be enough to supply to an entire local population for drinking water, agriculture, and industrial usage. Moreover, Haque, Rahman, and Samali (2016) evaluated climate change impacts on rainwater harvesting and concluded that the stored water would be reduced in the future due to the increase in variation patterns of precipitation. For these reasons, it is not enough to only have rainwater harvesting; hence solutions should also focus on reducing water loss cheaply and sustainably.

For cases like Yunnan, where the direct loss of water is due to fractured rocks, BioSealing is a relatively new technique that could solve this issue. BioSealing is a technique developed by Deltares (formerly known as GeoDelft) to seal leaks in water-retaining structures (Van Paassen, 2011). Essentially, this method injects nutrients to microorganisms, such as bacteria, that are naturally found in the soil and groundwater to stimulate biomass growth to seal the leaks (further explained in section 2.1.1). Lab and field experiments done by Deltares have shown that BioSealing works at 3D scale and in situ (Veenbergen, Lambert, van der Hoek, van Tol, & Weersma, 2005). They have also successfully applied BioSealing in pilot applications such as the dam seepage along the river Danube in Austria (Blauw, Lambert, & Latil, 2009).

The BioSealing terminology should not be confused with BioGrouting, another technique developed by Deltares as part of their SmartSoils program (Van Paassen, 2011). As mentioned before, BioSealing aims to seal leaks in water-retaining structures, whereas BioGrouting aims to strengthen granular soils. Both techniques use microorganisms, but they use different species and different nutrients. In literature, BioSealing is analogous to bioclogging; however, it was understood that Deltares wanted to patent their version of bioclogging as BioSealing to separate their technique from other similar ones such as the ones developed by Ross and Bickerton (2002) (Blauw et al., 2009). As previously noted, what separates BioSealing from the others is that this bioclogging technique is the first technique that has successfully achieved its aim at 3D scale and in situ.

Most of these BioSealing experiments and applications revolved around reducing seepage discharge in the subsurface to either repair water retaining civil constructions or repair

natural layers to prevent unwanted migration of contaminants (e.g., toxic substances and saltwater intrusion). It is believed that no existing studies are investigating the repair of subsurface fractured rock to saturate the overlying soil with (rain)water. In addition, lab experiments have only been done from a bottom-up approach where the nutrient was injected from the bottom side of the leak rather than from the top - at least from the accessible literature found from Deltares (Liao, Zhao, Lambert, & Veenbergen, 2007; Van Beek, Den Hamer, Lambert, Latil, & Van Der Zon, 2007; Veenbergen et al., 2005). The reason why a bottom-up approach was chosen for the lab experiments was to avoid preferential flow. As a result of this approach, all of the BioSealing experiments were done under saturated conditions, which is not representative of dryland conditions.

A top-down approach is needed as it helps simulate unsaturated conditions in dryland regions such as Yunnan. Moreover, if it were done from the bottom-up in real applications, it would require drilling into the fractured rock layer, which could further fracture the rock layer. There are concerns on whether BioSealing will develop at the right place (around the leak) if done in this manner. Two field applications have shown success in applying the BioSealing technique from a non-bottom-up approach, such as from left to right and top-down; however, they were done under saturated conditions (Admiraal & Molendijk, 2006; Blauw et al., 2009; Ross & Bickerton, 2002; van der Zaan, 2020). It is believed that what makes these lab and field applications successful in sealing at the correct areas is the presence of a converging steady state flow of water and nutrients in the porous medium towards the leak (Blauw et al., 2009; Van Paassen, 2011). For these reasons, it should be possible to do BioSealing in a top-down manner on a lab scale. To summarize, Figure 1.1 below illustrates the situation in dryland regions such as Yunnan and the desired outcome of applying BioSealing, which is to produce a groundwater table.

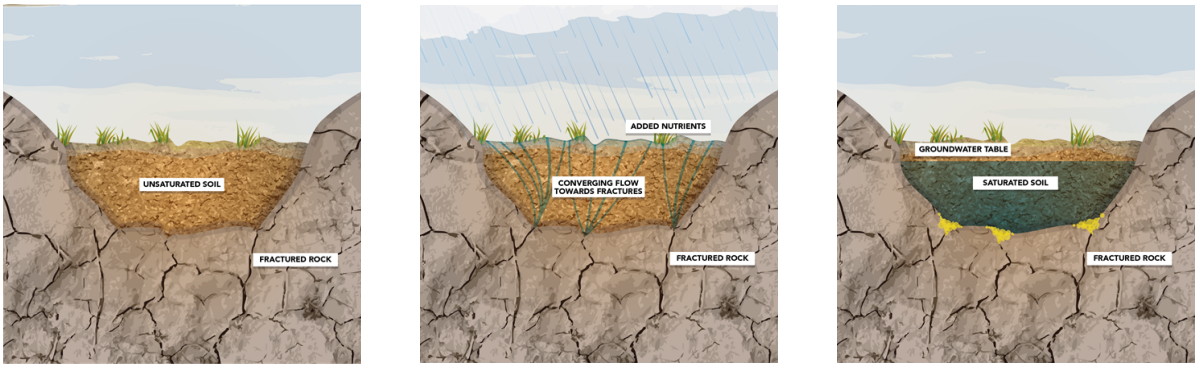


(a) Stage 1 (b) Stage 2 (c) Stage 3

Figure 1.1.: (a) No groundwater table present as water is seeped through the rock fractures; (b) BioSealing is applied in a top-down manner with a converging flow of water towards the fractures; (c) The fractures are sealed and a groundwater table is established (Schotting, n.d.).

## 1.3. Research Objective & Question

Lab experimental studies are needed first to see whether BioSealing fractured rock can help saturate the overlying soil with water before attempting field experiments and applications to solve the freshwater issue like in Yunnan. Thus, the objective of this research is to execute these lab experiments. This was done by designing and setting up sandbox-type experiments with the BioSealing technique from a top-down approach and measuring the flow and saturation distribution of water in the soil before and after applying it. A possible relationship can be found between the saturation distribution and the gap size of the fracture as a byproduct.

This research is theory-orientated, where it attempts to provide some novel knowledge on the BioSealing technique so that it can eventually be implemented in places like Yunnan. It follows that the main research question is:

"To what extent is the BioSealing technique effective in sealing a single hole fractured rock to establish a groundwater table in the overlying soil?"

To help answer this, the research question is delineated through these sub-questions:

1. What is the water saturation distribution before and after applying BioSealing?
2. What is the seepage flow rate before and after applying BioSealing?
3. Where did BioSealing occur in the sandbox setup?

# 2. Research Framework

This section of the thesis describes the relevant theories and concepts from BioSealing and bioclogging related literature and its relation to the research objective. It also discusses the scientific and societal relevance of this research.

## 2.1. Theoretical Framework

### 2.1.1. BioSealing Principles

Understanding the physical, chemical, and biological processes involved in the BioSealing technique is essential. In the BioSealing review article of Blauw et al. (2009) and Van Paassen (2011), they explained that the sealing process involved five steps and these steps are:

1. Bacteria fermenting the nutrients produce organic acids, resulting in a lowered pH due to redox reactions (Madigan, Martinko, & Parker, 1997).

2. The resulting higher acidity initiates (chemical and biological) weathering of fines (e.g., tiny mineral or organic particles) that are attached on larger grains (Štyriaková, Štyriak, Malachovskỳ, Večera, & Koloušek, 2007).

3. Since the bacteria are fed by a high level of nutrients in the ground, it triggers exponential bacterial growth and forms extracellular polymeric substances (EPS, otherwise known as biofilm). The majority of the bacterial growth occurs in the surrounding area of the leak since this is where the maximum flow rate is taking place, which results in a constant supply of nutrients.

4. The existing mobilized particles in the ground are entrapped by the formed EPS (funnel working) (Sutherland, 2001).

5. The injected nutrient also contains metal ions that initiate small clay particle flocculation and results in the sealing of the leak in the soil pores (Dontsova & Norton, 1999).

There are concerns about whether or not the sealing of the leak is durable enough against biodegradation of EPS and the stopped supply of nutrients. The lab and field experiments done by Veenbergen et al. (2005) have shown otherwise that the biofilm was still present in the surrounding area of the leak 4 months and 3 months later since the last injection of nutrients, respectively.

### 2.1.2. Decline in Flow Measurement

In bioclogging experiments, the key evidence that shows that clogging has taken place is the decline in flow in a column from its initial flow before clogging (Abdel Aal, Atekwana, & Atekwana, 2010; Engesgaard, Seifert, & Herrera, 2006; Liao et al., 2007; Ross, Villemur, Deschênes, & Samson, 2001; Seifert & Engesgaard, 2007, 2012; Seki, Suko, & Miyazaki, 2002; Van Beek et al., 2007; Veenbergen et al., 2005; Zhong & Wu, 2013a; Zhong, Wu, & Xu, 2013b). There is a difference in how the decline in flow is presented in the literature, particularly how the BioSealing experiments determined it compared to the others. Nevertheless, they are all derived from Darcy's equation of flow:

$$Q = A * K * \frac{\Delta h}{\Delta z} \tag{2.1}$$

where $Q$ = flow rate [$L^3$/T], $A$ = cross-sectional area of the column [$L^2$], $K$ = hydraulic conductivity [L/T], $\Delta h$ = hydraulic head difference across the column layer [L] and $\Delta z$ = the height difference across the column layer [L]. The most common way that bioclogging experiments have measured the flow decline is the decline in hydraulic conductivity over time, a rearrangment of equation (2.1), as shown in the experiments of Seki et al. (2002), Abdel Aal et al. (2010), and Zhong and Wu (2013a):

$$K = \frac{Q}{A} * \frac{\Delta z}{\Delta h} \tag{2.2}$$

The characterization of the decline in flow can become more complex by redefining equation (2.2). For example, Seifert and Engesgaard (2007) defined the decrease in hydraulic conductivity by relating it to biological growth in pores. They first described that the pore volume could be divided into mobile and immobile domains, where the immobile domain is the biomass:

$$\phi = \phi_{bio} + \phi_m \tag{2.3}$$

where $\phi$ = total porosity, $\phi_{bio}$ = the biomass porosity (immobile) and $\phi_m$ = the mobile porosity. The accumulation of biomass means that the mobile porosity will decrease, ultimately affecting the soil permeability. It follows that the relative mobile porosity is described by:

$$\beta = \frac{\phi_m}{\phi} \tag{2.4}$$

where $\beta$ = the mobile porosity fraction. Seifert and Engesgaard (2007) then presented two models that connect the hydraulic conductivity with the changes in the mobile porosity domain: (1) the parametric model and (2) the pore network model. Full details of the two model applications can be found in their article, but the parametric model equation is illustrated here:

$$\frac{K(\beta)}{K_{ini}} = \beta^c \quad for \quad \beta > \sqrt[c]{\frac{K_{min}}{K_{ini}}} \tag{2.5}$$

where $K$ = hydraulic conductivity, $K_{ini}$ = initial hydraulic conductivity, $K_{min}$ = minimum threshold value for the hydraulic conductivity, and $c$ = an exponent that differs amongst the various models.

In BioSealing experiments, on the other hand, they took a different approach and interpreted the decline in flow as the reduction of soil permeability. They defined it by the clogging factor, C (Liao et al., 2007; Van Beek et al., 2007; Veenbergen et al., 2005):

$$C = \frac{(\frac{\Delta Q}{\Delta h})_{t=0}}{(\frac{\Delta Q}{\Delta h})_{t=t}} \tag{2.6}$$

where $\Delta Q$ = decline in flow [$L^3$/T] and $\Delta h$ = difference in hydraulic head between two manometers [L].

### 2.1.3. BioSealing Effects

In the literature review of bioclogging by Baveye, Vandevivere, Hoyle, DeLeo, and de Lozada (1998), they noted that the decline in flow from bioclogging experiments followed a particular pattern of four phases. Using an example from the research of Okubo and Matsumoto (1983), the four phases are: (1) An initial decrease in flow, (2) then a transition phase occurs where the decline in flow would stop, and the flow starts to increase slightly again. (3) After this transitional period, the flow decreases until (4) it levels off, as shown in Figure 2.1.

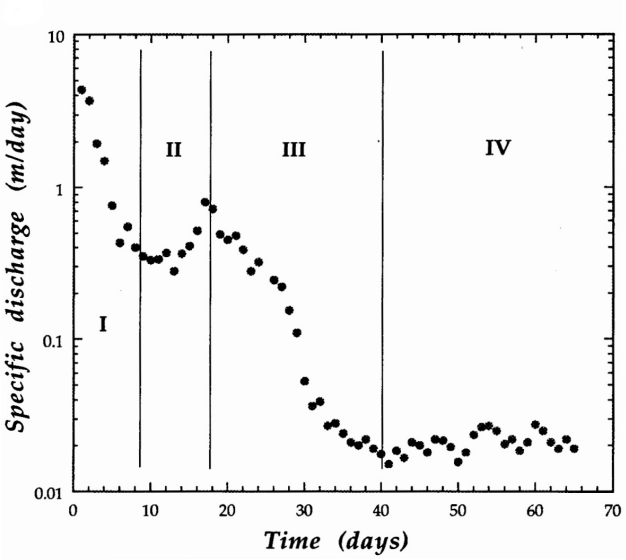


Figure 2.1.: The decline in flow pattern due to bioclogging: (1) an initial decrease, (2) transitional phase of a stopped decline in flow followed by a slight increase, (3) decline in flow continues and (4) the flow levels off (Baveye et al., 1998).

Some bioclogging research did not exhibit one of the first two phases. That was expected because of the various ways the decline in flow was quantified and the different

nature in how bioclogging developed in each experiment (Baveye et al., 1998). These patterns can still be seen, especially the last two phases, in relatively recent bioclogging research, including BioSealing (Abdel Aal et al., 2010; Liao et al., 2007; Ross et al., 2001; Seifert & Engesgaard, 2012; Seki et al., 2002; Van Beek et al., 2007; Veenbergen et al., 2005; Zhong & Wu, 2013a). The changes seen in the last two phases appear to be of an exponential decline, and Zhong and Wu (2013a) characterized it (in terms of hydraulic conductivity) as:

$$K = K_0 * exp(-bt) \tag{2.7}$$

where $K$ = the hydraulic conductivity in the soil column, $K_0$ = the initial hydraulic conductivity, $t$ = time, and $b$ = an unknown fitting parameter. Since BioSealing experiments measure the changes in clogging factor over time with equation (2.6), the resulting pattern is not an exponential decline but an exponential increase (Figure 2.2) (Liao et al., 2007).

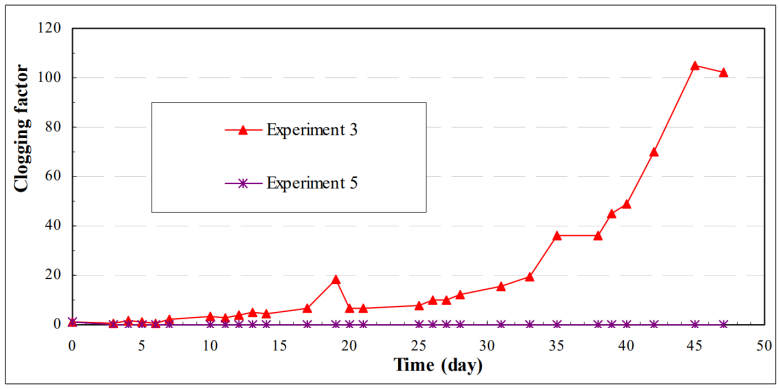


Figure 2.2.: The exponential increase in clogging factor over time in experiment 3 (with nutrients) and no increase in experiment 5 (without nutrients) from the BioSealing research of Liao et al. (2007).

Different BioSealing experiments reported various clogging factor results within the same time frame of 6 weeks after the initial injection of nutrients (Table 2.1). These differences occur due to how their experiments were set up. For example, they used different nutrient injection frequencies and duration. Completely sealing the leak is unnecessary, as long as the leakage does not influence the function of the water-retaining structure or its failure (Blauw et al., 2009; Van Paassen, 2011).

For this study, a potential and desirable outcome after applying the BioSealing technique to seal a fractured bedrock is the saturation of the overlying topsoil. Saturation is defined as the proportion of pores that consists of water (Dingman, 2015):

$$S = \frac{V_w}{V_p} = \frac{V_w}{V_a + V_w} = \frac{\theta}{\phi} \tag{2.8}$$

where $V_w$ = volume of water, $V_p$ = volume of pores in the soil, $V_a$ = volume of air, $\theta$ = water content, and $\phi$ = porosity. Saturation is a good measure to see whether

a groundwater table is established or risen in the unsaturated zone of the subsurface. Although the main effect of BioSealing is the decline in flow, the groundwater table establishment can be understood as a secondary effect of it.

Table 2.1.: The various reported clogging factor from BioSealing experiments, lab and field.

| **Experiment Type** | **Clogging Factor** | **Source** |
|---|---|---|
| Lab | 100 | Liao et al. (2007) |
| Lab | 20 | Veenbergen et al. (2005) |
| Lab | 250 | Van Beek et al. (2007) |
| Field | 5 | Veenbergen et al. (2005) |

## 2.2. Conceptual Framework

To summarize what was discussed so far, a conceptual framework is created to visually explain how the theories are connected to the research objective, as shown in Figure 2.3. Without the intervention of BioSealing, the current situation, such as in Yunnan, will continue where water that enters the subsurface from rain will flow through the fractured bedrock. This results in little to no groundwater table, further contributing to land degradation (Figure 2.3a).

When BioSealing is applied, it is expected that the fractures in the bedrock will be sealed, causing a low flow through the leak, which would yield saturated topsoil, thus helping in the restoration of degraded land (Figure 2.3b). It is hypothesized that there is some form of cause and effect relationship between the fracture size (independent variable), the flow through the leak (dependent variable), and the saturation distribution (dependent variable). BioSealing is the moderator variable as it alters the effect that the fracture size has on the flow and the saturation distribution because it seals the fracture. These variables were what this study has focused on, as highlighted by the red outline in Figure 2.3b. Sub-question 1 is linked with the dependent variable of saturation. Sub-question 2 is related to the dependent variable of flow, and sub-question 3 is connected to the independent variable of fracture size.

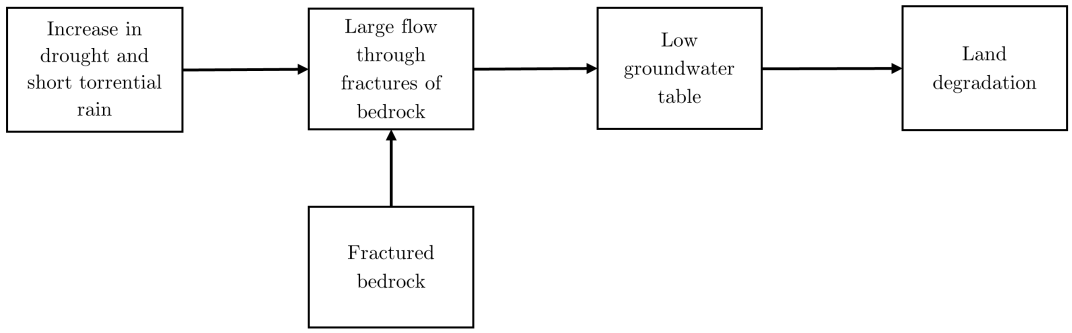


(a) The current situation in certain dryland regions like Yunnan without the intervention of BioSealing

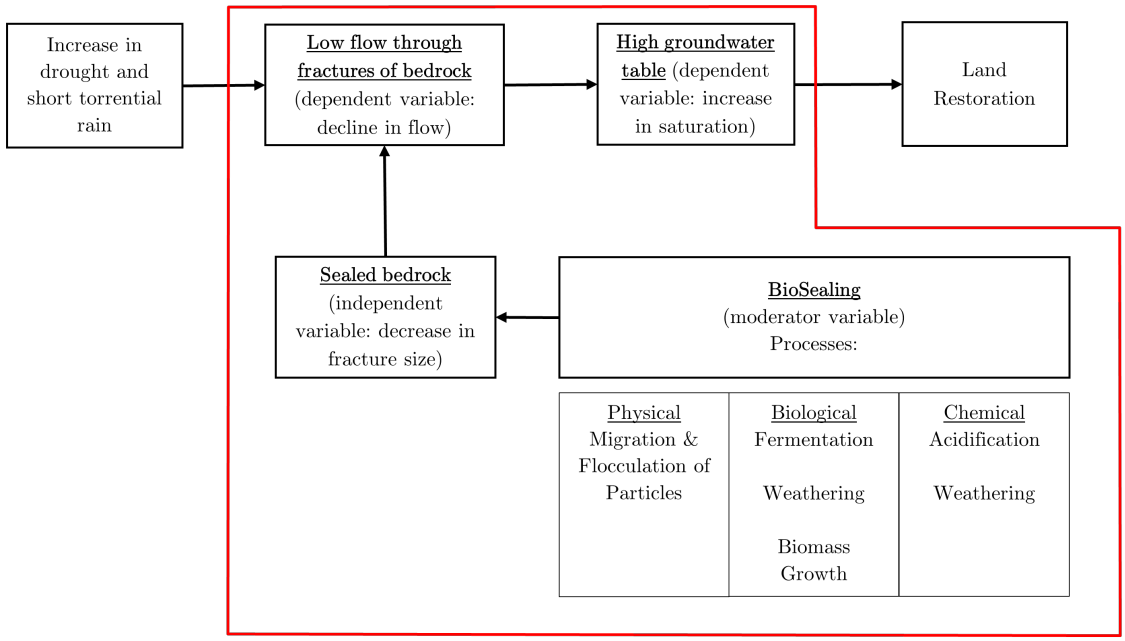


(b) The hypothesized outcome when BioSealing is applied. The red outline highlights the focus area and the variables of this research

Figure 2.3.: The conceptual framework linking the BioSealing theory to the research objective

## 2.3. Relevance

As previously discussed, this research hopes to produce novel knowledge towards the BioSealing technique in terms of sealing fractured rocks to establish a groundwater table in the overlying soil. Scientifically, this research indirectly determines if there is a relationship between fracture size and saturation distribution. This will illustrate how much of the fracture size is needed to produce a groundwater table. At the same time, this research can potentially further validate the results of Veenbergen et al. (2005), Liao et al. (2007), Seki et al. (2002), and Zhong et al. (2013b), regarding the BioSealing effect

of reduced soil permeability and flow. It will also further prove that BioSealing can be done in a top-down manner under unsaturated conditions. If this investigation is successful, field-scale experiments can be done and eventually applied to real applications such as Yunnan.

Societal benefits can be seen when BioSealing solves the freshwater issue seen in Yunnan and other similar dryland regions. During wet periods, a groundwater table can be established near the surface, and this would help provide soil moisture for vegetation to grow. The roots and the organic matter from the resulting vegetative growth can give strength and structure to the soil to be less vulnerable to land degradation. This restored land could potentially be helpful for rainfed agriculture. A secondary effect of this is that there is less reliance to use harvested rainwater for agriculture and could be better used for domestic purposes such as potable water. It follows that this research is aligned with some of the Sustainable Development Goals (SDGs).

The SDGs are goals developed by the United Nations that act as the blueprint for all countries to attain a more sustainable future (United Nations, n.d.). The main SDGs that this research hopes to achieve in the future are SDG 6 (clean water and sanitation) and SDG 15 (life on land). Specifically, the following targets from both SDGs that are hoped to achieve are conveyed in Table 2.2.

Table 2.2.: The targets that is hoped to achieve from SDG 6 and SDG 15 (United Nations, n.d.)

| **SDG** | **Target** |
|---|---|
| 6: Clean Water & Sanitation | 6.4: By 2030 substantially increase water-use efficiency across all sectors and ensure sustainable withdrawals and supply of freshwater to address water scarcity and substantially reduce the number of people suffering from water scarcity |
| 15: Life on Land | 15.3: By 2030, combat desertification, restore degraded land and soil, including land affected by desertification, drought and floods, and strive to achieve a land degradation-neutral world |

# 3. Materials & Methods

This research aimed to see the effectiveness of the BioSealing technique from a top-down approach by investigating the cause and effect relationship between the sealing of the leaking hole, the flow through it, and the saturation distribution of the overlying topsoil. To achieve this, primary quantitative data were needed by gathering experimental data. This section of the study explains the details of how the data were collected and analyzed.

## 3.1. Experimental Setup

### 3.1.1. The Overall Setup

The overall setup of the experiment is shown in Figure 3.1. There were four 10 L glass vessels where two of them contained water (blue) and the other two contained diluted nutrients (orange) (1). One water vessel and one nutrient vessel were connected through a three-way valve to switch between the two liquids (2). They were then connected via silicon tubes to a peristaltic pump to control the flow rate (3). The tubes were further connected to a PVC plate attached above the PVC tank to hold the tubes in place (4). Five small tube connectors were attached to each tube to allow water to drip from them into the tank (5), where the inner dimensions of the tank were 10x60x60 cm. The soil was packed until height 50 cm of the tank so that there is 10 cm left of the tank unfilled in case a pool of water develops on top of the soil. A 2 cm thick PVC plate with a square leakage hole at the center was placed at height 10 cm of the tank to simulate a fractured bedrock (6). The leakage hole had a dimension of 5x5 cm where water flowed through it.

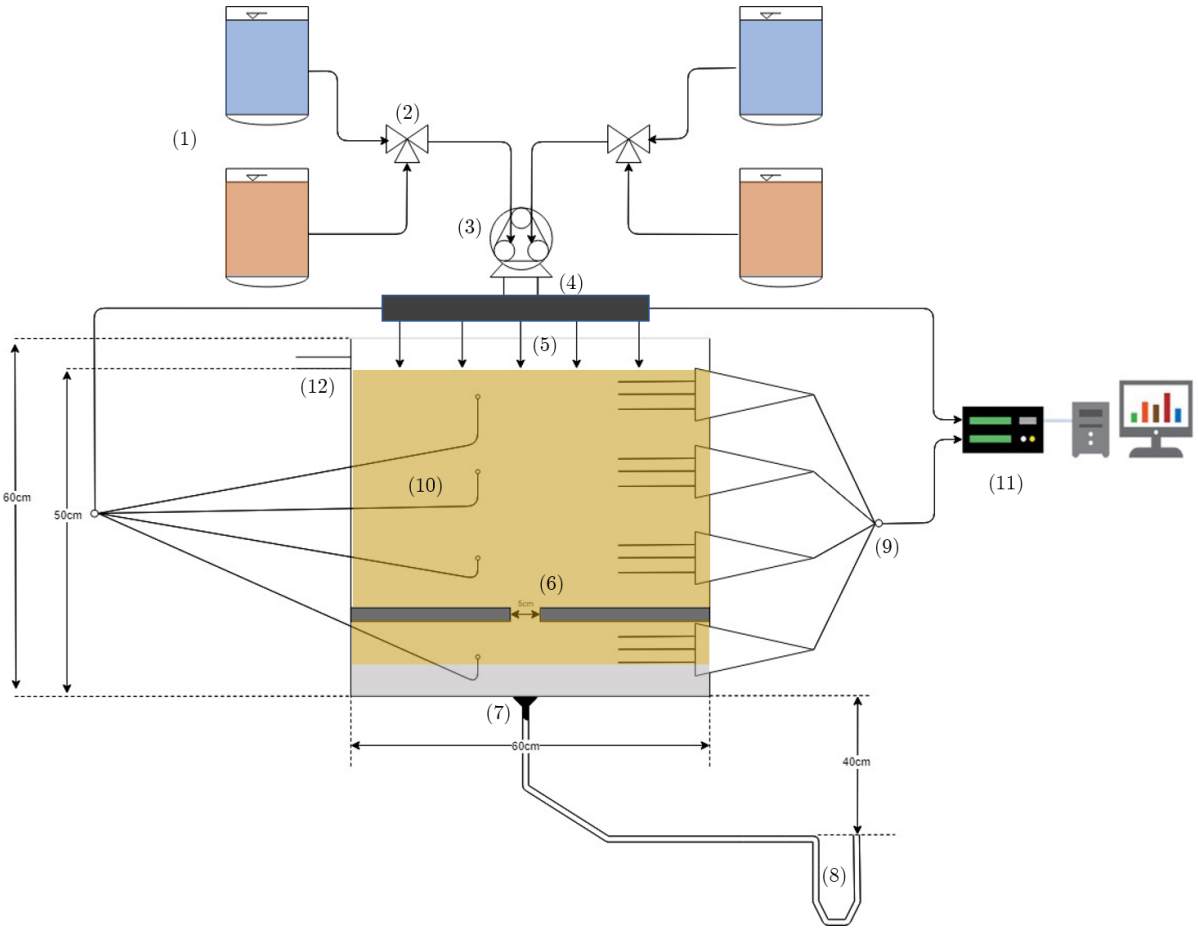


Figure 3.1.: Schematic diagram of the experimental setup, numbers indicating various components: (1) vessels containing either water (blue) or diluted nutrients (orange), (2) three-way valve to switch between water and nutrients, (3) peristaltic pump, (4) plate to hold tubes, (5) fluid dripping points, (6) leakage plate with a 5x5 cm hole, (7) screw-like coupling, (8) outlet tube shaped like a siphon, (9) 5TE sensors, (10) tensiometers, (11) data logger connected to a computer and (12) second outlet

At the bottom of the tank was a 10 cm diameter hole attached to a screw-like PVC coupling containing a hydrophilic membrane to prevent air from entering the tank system (7). The outlet of the coupling is then connected to a tube with an inner diameter of 75mm. This tube was shaped as a siphon where a water reservoir sat inside it and was situated 40 cm below the outlet (8). The siphon served two purposes: to create a constant negative pressure to simulate unsaturated conditions, and the other was to suck water from the tank quicker than normal free drainage.

Four 5TE sensors were attached on the right side of the tank (9), and four tensiometers were attached on the front side of the tank, just left off the center (10). These sensors sent electrical signals to a data logger connected to a computer to monitor and record the data from the tank (11). An outlet was installed at the top of the tank (12) during the experiment due to a pool of water developing on top of the soil, which needed to

be removed. The overall setup was situated between the gamma system to record data of the tank system also. The coordinate locations where the sensors and the gamma measurements were taken are conveyed in Table 3.1 when the reference level is taken at the center of the soil surface.

Table 3.1.: The coordinate locations of where the measurements were taken for the 5TE sensors, tensiometers and gamma rays

| **Devices** | **Coordinates (cm)** |
|---|---|
| 5TE Sensors | (30, -5), (30, -20), (30, -35), (30, -46.5) |
| Tensiometers | (-10, -5), (-10, -20), (-10, -35), (-10, -46.5) |
| Gamma Rays | (5, -5), (5, -20), (5, -35), (5, -46.5) |
| | (15, -5), (15, -20), (15, -35), (15, -46.5) |

### 3.1.2. Soil Material & Packing

The soil used in this experiment was collected from the topsoil of Griftpark, Utrecht. An analysis of the physical and hydraulic properties of the soil was done by Cecchetto (2021) using HYPROP, Graduation Test, and Thermogravimetric analysis. Results of the relevant properties are shown in Table 3.2. Cecchetto (2021) noted a mismatch of the $K_s$ value from the HYPROP analysis and the tank system, where the $K_s$ value was significantly lower than what was observed in the tank. For this study, the value from the tank system was chosen as it was a better representative. The average porosity from the HYPROP analysis was also revised to the value of the tank system.

Table 3.2.: Properties of the soil used (Cecchetto, 2021)

| **Property** | **Value** |
|---|---|
| D50 - mean particle diameter [mm] | 0.33 |
| $\rho_b^d$ - dry bulk density [g/cm$^3$] | 1.61 |
| $\rho_s$ - density of solid substance [g/cm$^3$] | 2.65 |
| $K_s$ - saturated conductivity [cm/hr] | 1.89 |
| $\phi$ - average porosity [-] | 0.45 |
| Organic matter content | 7% |

Before packing the soil into the tank, the holes where the tensiometers and 5TE sensors will be placed were covered with tape to avoid any loss of soil Cecchetto (2021). The bottom section of the tank below the seepage plate was packed first. A nylon mesh was first placed at the bottom so that no soil material falls out of the outlet hole. A layer of pebbles and a layer of gravel on top were packed before the actual soil to prevent bioclogging at the outlet. Next, the soil was partially saturated before filling the tank with it - to form a mud paste consistency to reduce the possibility of having air trapped in the pore spaces and preferential flow path formations. 2cm layers of soil were then

added and pressed with a custom-made pestle to achieve field density. By using sharp prongs, the soil surface was raked and scratched to avoid horizontal layering.

Once the bottom section was filled, the seepage plate was carefully installed and the leaking hole was then filled with soil. The top section of the tank above the seepage plate followed the same packing procedure and it was packed until height 50cm so that a 10 cm gap between the soil surface and the top of the tank was created in case a pool of water develops, as previously stated. A mesh was placed on top of the soil surface to distribute water from the dripping system further. The tapes covering the holes for the sensors were removed and by using a needle, the soil was poked to create tiny holes for easy insertion of the sensors. Lastly, silicon glue was applied during the insertion of the sensors to seal off any gaps.

### 3.1.3. Water & Nutrient Injection

The fluids involved in this experiment were water and diluted nutrients. The brand of nutrients used is called Nutrolase, a protamylasse from the waste product of processed potato made by AVEBE. The nutrients were diluted with water at a proportion of 1:4. Before the nutrients were injected into the tank, a steady-state flow of water was established first to remove any remaining air in the soil and obtain an initial outflow measurement. The flow rate was kept constant at 120 ml/hr initially but switched to 36 ml/hr when a pool of water on top of the soil developed. Once the steady-state flow was achieved, the diluted nutrients were injected twice a week, then increased to three times per week when the effluent flow rate showed no decline. On injection days, the nutrients were injected for about 15 to 16 hours during the night, then switched to water in the morning.

## 3.2. Data Collection

### 3.2.1. Outflow

The outflow of the tank effluent was measured twice every morning and averaged. The effluent tube from the bottom of the tank was connected to a graduated cylinder where water was flown into and the mass of water was measured using a weighing scale. This was done per hour to obtain a value in the units of [ml/hr]. This measurement was useful to answer sub-question 2 as it indicated whether BioSealing had taken place or not because a decline in flow is expected.

### 3.2.2. Pressure Head

The pressure heads of the tank system at the various depths (z = 5, 20, 35, and 46.5cm) were measured using tensiometers created by Rhizo Instruments (Figure 3.2). At the tip of the tensiometer is a permeable cup (a) which allows water from the pores of the soil to enter a water-filled pipe (b). When no flow was present, the tension between the

soil and the pipe was in equilibrium. The pressure head of the tank was determined by the pressure in the pipe relative to the existing pressure of the small chamber (c). To maintain a constant pore suction pressure in the tensiometer, a 10 ml syringe was used to create a vacuum chamber (d) close to -1 atm. The pressure transducer (c) measured the pressure and sent electrical signals to the data logger (e), where the pressure is recorded over time. The tensiometers were horizontally inserted into the tank for better precision of measurements. The tensiometers were calibrated before the experiment started by using the hanging water column method. Results of the calibration can be found in Appendix A.

The pressure head measurements were used to calculate the clogging factor, as shown in equation (2.6). The pressure head differences over time helped indicate the decline in flow, which shows that BioSealing has taken place at different depths. It follows that it helped in answering sub-question 2 and 3. The measurements also served as an indicator of whether a groundwater table is established, as well as its location in the tank by observing when the pressure is equal to 0 cm.

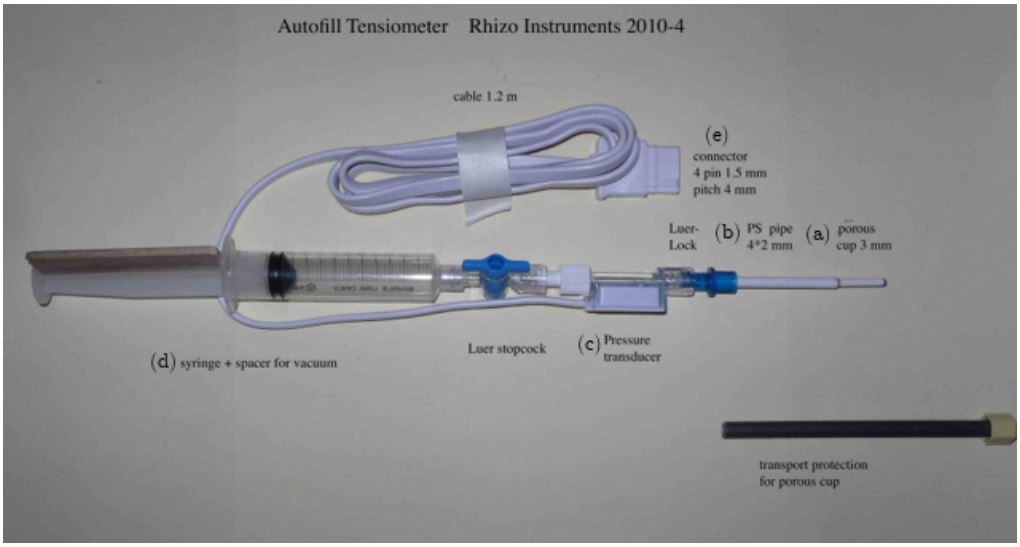


Figure 3.2.: The autofill tensiometer used - developed by Rhizo Instruments

### 3.2.3. Volumetric Water Content

5TE sensors made by Decagon Devices (Figure 3.3) were used to measure the volumetric water content ($\theta$) at different depths (z = 5, 20, 35, and 46.5cm). To determine the water content, the dielectric permittivity ($\epsilon$) of the surrounding medium was measured via an electromagnetic field (Meter Group, 2018). 70 MHz oscillating wave was supplied by the sensors to the prongs in which it charges with the dielectric permittivity of the material. Each material exhibits different dielectric permittivity; for instance, soil has a dielectric permittivity of approximately between 2 and 5, whereas air is 1. The permittivity of water is 80, which illustrates that it can contain more charge than the other materials. Since the charge in the soil remains constant and that air has almost no charge, any

changes in the dielectric permittivity readings are linked to the changes in the water content in the soil (Campbell, 2014). The equation of Topp was then used to convert the raw dielectric permittivity data from the sensors to volumetric water content (Meter Group, 2018; Topp, Davis, & Annan, 1980):

$$\theta = 4.3 * 10^{-6} * \epsilon^3 - 5.5 * 10^{-4} * \epsilon^2 + 2.92 * 10^{-2} * \epsilon - 5.3 * 10^{-2} \tag{3.1}$$

The recorded water content contributed to answering sub-question 1, which was later converted to saturation (section 3.3.2). The changes in water content in the tank system helped identify when and where there was an increase in water table height during the experiment. It also served as an indicator of whether an unsaturated steady-state flow system was achieved or not.

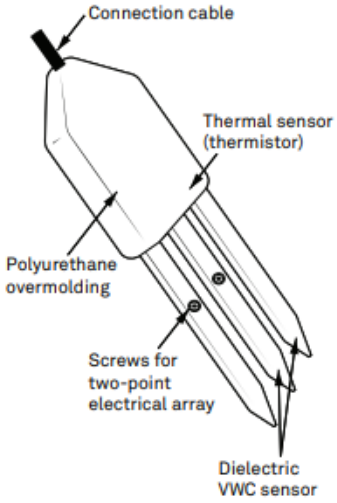


Figure 3.3.: The 5TE sensor and its components (Meter Group, 2018)

Despite it not contributing directly towards the sub-questions, the bulk electrical conductivity (ECb) was monitored from the 5TE sensors as well. ECb is the electrical current that a material transmits, which means that in the tank system, the soil, water, and nutrients influence the ECb. For example, if there is an increase in water content or nutrients, the ECb will also increase. This measurement was mainly used to track the presence of the nutrients at each depth to know whether it has reached the leakage hole depth. The ECb results can be found in Appendix C.

### 3.2.4. Gamma Intensities

Another way to determine the saturation of the tank is the gamma-ray transmission method. This system uses two radioactive sources to emit gamma rays, namely Cesium 137 and Americium 241. The gamma rays are emitted through an opening source of 6mm in diameter with an energy peak of 59 keV and 662 keV for $^{241}$Am and $^{137}$Cs, respectively. The intensities of both radioactive sources will decrease as the gamma rays are absorbed while traveling through the tank. A detector is placed opposite the source

where it measures the remaining intensities. These measured intensities can be defined by Beer-Lambert's law (Oostrom, Hofstee, Dane, & Lenhard, 1998):

$$I^j = I_0^j * exp(\sum_{i=1}^{n} -\mu_{ji} * \rho_i * \theta_i * x) \tag{3.2}$$

where $n$ = number of components, $i$ = the material phase i.e. solids and water, $j$ = the radioactive source, $I$ = measured intensity [1/T], $I_0^j$ = reference intensity [1/T], $\mu_{ji}$ = the mass attenuation coefficient [$L^2$/M], $\rho_i$ = the mass density [M/$L^3$], $\theta_i$ = the volumetric content of component $i$ and $x$ = the path length of the gamma beam through the tank. Sometimes, it is convenient to take the product of $\mu_{ji}$ and $\rho_i$ to obtain the volumetric attenuation coefficient $U_{ji}$ [1/L]. Thus equation (3.2) becomes:

$$I^j = I_0^j * exp(\sum_{i=1}^{n} -U_{ji} * \theta_i * x) \tag{3.3}$$

To measure the changes in water content in the tank system, the law of Beer-Lambert in equation (3.3) becomes equation (3.4) for unsaturated conditions:

$$I^j = I_0^j * exp(-U_{js} * \theta_s * x - U_{jw} * \theta_w * x) \tag{3.4}$$

where $U_{js}$ = the soil attenuation coefficient, $U_{jw}$ = the water attenuation coefficient, $\theta_s$ = volume fraction of solids, and $\theta_w$ = water content. For this study, it was favorable to take the product of the volume fraction ($\theta$) and the path length of the tank ($x$) to get values of the path length of the soil ($x_s$ [L]) and water ($x_w$ [L]) of the gamma-ray. This was to calculate the saturation, such as in the research of Zhuang (2017) and Badi (2018). It follows that equation (3.4) turns into:

$$I^j = I_0^j * exp(-U_{js} * x_s - U_{jw} * x_w) \tag{3.5}$$

The calibration of the gamma system and the determination of the attenuation coefficients $U_{js}$ and $U_{jw}$ were done beforehand. The results are shown in Appendix B.1 and Appendix B.2, respectively. The details of the procedure to calibrate and obtain the attenuation coefficients are given by Oostrom and Dane (1990).

The raw intensity data obtained from the gamma-ray transmission method helped with answering sub-question 1. More attenuation in the intensities relative to the reference intensity indicates more water being present in the tank system. Less attenuation means less water in the tank. The intensities were measured once per day but taken three times and averaged.

### 3.2.5. Soil Sampling for Bacterial DNA

The bacterial DNA found in the tank system due to biomass growth from BioSealing was collected for 16S rRNA gene count analysis. Soil samples were taken at different locations from the tank based on a 4x6 grid (Figure 3.4), where each cell location has its code. The cells are also colored to represent the depth interval they were sampled

from. They were first stored at -20 °C until Deltares collected them for DNA isolation and 16S gene quantification. Soil sampling for bacterial DNA in the tank contributed to determining sub-question 3. The presence or lack of DNA in particular locations of the tank illustrates whether BioSealing took place in the right area or not.

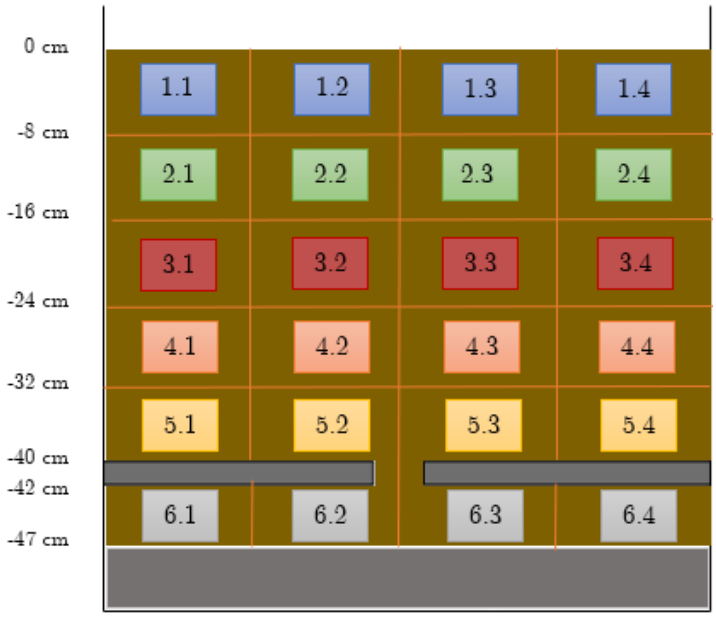


Figure 3.4.: The sampling locations of the tank for bacterial DNA. Each cell is labelled with its own code and coloured to reflect the depth interval they was taken from: (Blue) 0 to -8cm, (Green) -8 to -16cm, (Red) -16 to -24cm, (Orange) -24 to -32cm, (Yellow) -32 to 40cm and (Grey) -42 to -47cm.

## 3.3. Data Analysis

### 3.3.1. Decline in Flow

The effluent flow rate measurements were used to create a graph of the effluent flow rate versus time to illustrate how the flow declined over time. The flow measurements and the pressure head data were used to calculate the clogging factor using equation (2.6) to determine the effectiveness of the BioSealing and where BioSealing occurred the most in the tank setup. This contributed to answering sub-question 2 and 3.

### 3.3.2. Saturation

The raw volumetric water content data from the 5TE sensors were converted to saturation using equation (2.8). To calculate the saturation from the measured intensities, $x_s$ and $x_w$ were determined first from equation (3.5). The reference intensity $I_0$ was set equal to the measured intensity of the empty tank. Once determined, the following equation from Zhuang (2017) was used to calculate the saturation:

$$S = \frac{x_w}{x - x_s} \tag{3.6}$$

Plots of the saturation versus time were created for each measured location. This would illustrate the changes in saturation due to the decline in flow through the leak caused by BioSealing. This helped in answering sub-question 1.

### 3.3.3. Bacterial Count

To do a bacterial count using their 16S rRNA genes, the DNA must be isolated first from the soil. Exact details of the procedure to do so were not given by Deltares, but it follows similarly to the research of Ritalahti et al. (2006) by using a DNA isolation kit. The soil samples were first pelleted by centrifugation before using the kit. A buffer, enzyme, and peptidase were added to the bacterial pellet and then incubated. A proteinase was added next and further incubated. After incubation, DNA was eluted by using a buffer. A nested-PCR amplification method was then used to determine the existence of 16S genes in the sample. Once determined, the total bacterial count from their genes was ascertained twice using a TaqMan-based qPCR approach, which supported in answering sub-question 3. The gene count was then analyzed per cell and per layer. Anomalies in data were kept when analyzing the gene count per cell but omitted for the gene count per layer analysis.

## 3.4. Justification of Methodological Choices

### 3.4.1. Experimental Setup

To accurately simulate real-life conditions, the size of the tank setup needed to be as big as possible; however, it had to fit within the dimensional limits of the gamma system as well, hence why the dimensions of the tank were 10x60x60 cm. The decision to inject water and nutrients by dripping them rather than, for example, directly inserting tubes into the soil, was to facilitate an unsaturated steady-state flow. By doing so, the flux through the soil system is partly defined by the soil surface infiltration rate than the pump flow rate.

Natural soil was used instead of using clean sand or glass beads like in most subsurface hydrological studies. They are more representative of field conditions and that there are already existing microorganisms within the soil. Soil inoculation of microorganisms would be required if clean sand and glass beads were used.

### 3.4.2. Data Collection & Analysis

In BioSealing experiments such as Veenbergen et al. (2005) and Liao et al. (2007), they opted to use manometers to measure the pressure head in their setup which was suitable for them as they were doing their experiments under saturated conditions. Since this study aimed to have unsaturated conditions, manometers were not suitable as they

cannot measure negative pressure heads. Tensiometers developed by Rhizo Instruments were used instead as they can record both positive and negative pressure heads, as shown in the research of Biekart (2018) and Witte (2017).

There are a few ways to measure water content within a soil system, but to measure water content without being invasive during the BioSealing process limits options to using the gamma-ray transmission method as it does not require a device to be inserted into the tank. However, it was still useful to use devices, such as 5TE sensors to measure the water content for comparisons. Time domain reflectometry (TDR) devices were another option to measure the water content, like in the study of Mostafa and Van Geel (2012) and Rockhold, Yarwood, Niemet, Bottomley, and Selker (2005), but is limited to just that measurement. In contrast, the 5TE sensors can record other valuable data such as the ECb. Both the gamma-ray transmission method and the 5TE sensors are viable ways to monitor water content, as illustrated in the experiments of Zhuang (2017) and Biekart (2018), respectively.

To show that BioSealing occurred near the surrounding area of the leak, Veenbergen et al. (2005) and Liao et al. (2007) relied on using the clogging factor analysis of the decline in flow per layer depth, as well as a qualitative analysis of the soil. To further validate these results, a bacterial count approach similar to the research of de Jong (2020) and Mostafa and Van Geel (2012) was also taken for this study.

# 4. Results

This chapter details the outcome of the experiment and is structured according to the sub-questions of this research.

## 4.1. Sub-Question 1: Saturation Distribution

In sections 4.1.2 until 4.1.5, the saturation data at various depths have three types: (1) gamma central, (2) gamma off central, and (3) 5TE sensors. These three saturation measurements were taken at different tank locations (see Table 3.1) and represent the local behavior of that location. The gamma central data is located near the middle of the tank, whereas the gamma off central data was between the middle of the tank and the side of the tank where the 5TE sensors are situated.

### 4.1.1. Saturated Tank

Before the nutrients were injected, an unsaturated steady-state flow needed to be established first. In less than 4 days, the tank became fully saturated (Figure 4.1). Full saturation was achieved at 35cm depth (grey line) less than a day since the water dripping started. After 2 days of dripping water, full saturation was achieved at depth 20cm (orange line). At the same time, saturation at 35cm slowly declines. The 5cm (blue line) depth became fully saturated after 3 days of dripping. Depth 35cm continues to decline slowly, as well as at depth 20cm. It follows that water does travel towards deeper depths, but it accumulates over time and the water table rises. There is a minimal increase at depth 46.5cm (located below the leaking plate - yellow line) over time, but it never reaches full saturation as it only increased from 0.493 to 0.503.

As a result of the saturation of the tank, a pool of water developed on top of the soil. An outlet was installed at the top of the tank to drain it away. Establishing an unsaturated steady-state flow was no longer possible at this point of the experiment, so a decision was made to continue with a saturated steady-state flow.

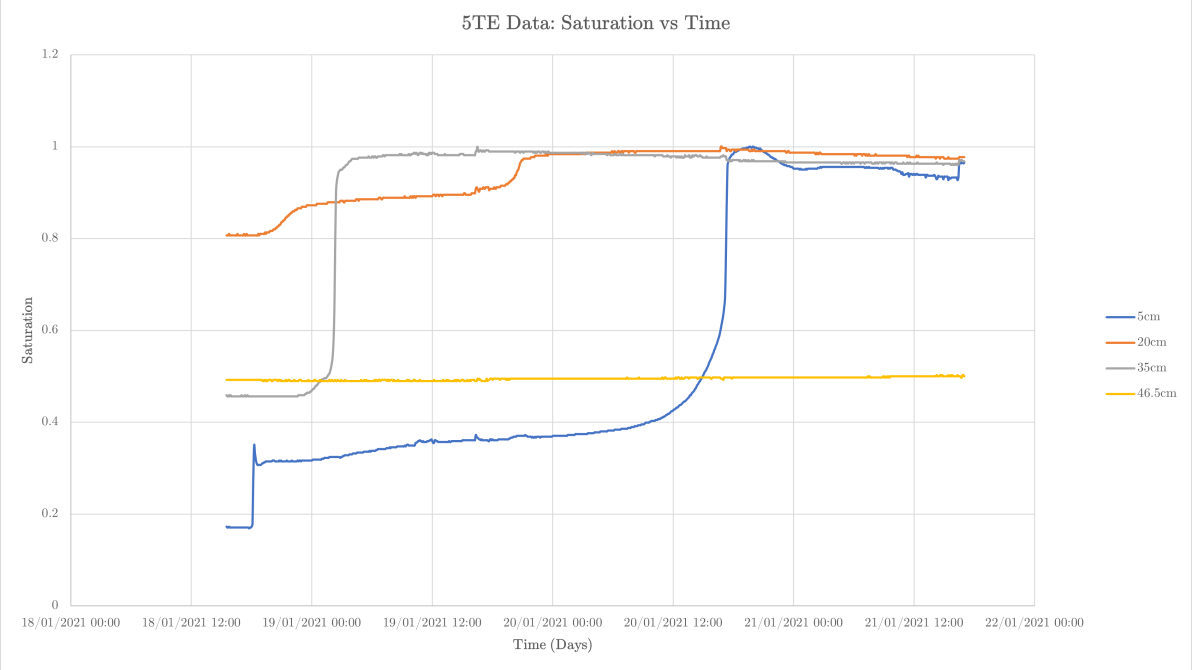


Figure 4.1.: The saturation data from the 5TE sensors at various depths illustrating the the tank became fully saturated in less than 4 days. Depth 5cm is the blue line, 20cm in orange, grey is depth 35cm and the yellow line is depth 46.5cm

### 4.1.2. Depth -5cm

The saturation at depth -5cm between the gamma and 5TE sensor results are illustrated in Figure 4.2. The blue line represents the gamma central data, the orange line is the gamma off central data and the 5TE sensor is the grey line. The vertical orange lines illustrate when the nutrients were injected. Before the start of the nutrient injection, the soil was close to full saturation. Then, from 10/02 until 12/02, the saturation decreased in both the gamma and sensor data, except for the sensor on 11/02, where there was an increase. The saturation then increased afterward for the gamma data and remained relatively constant, barring the gamma off central data on 17/02 as there was a sudden decrease. For the 5TE data, the saturation remained constant then increased from 29/02 onward. All three data types ended with about the same saturation at approximately 0.86. It was expected that the saturation would remain close to full saturation throughout time, but these results show otherwise.

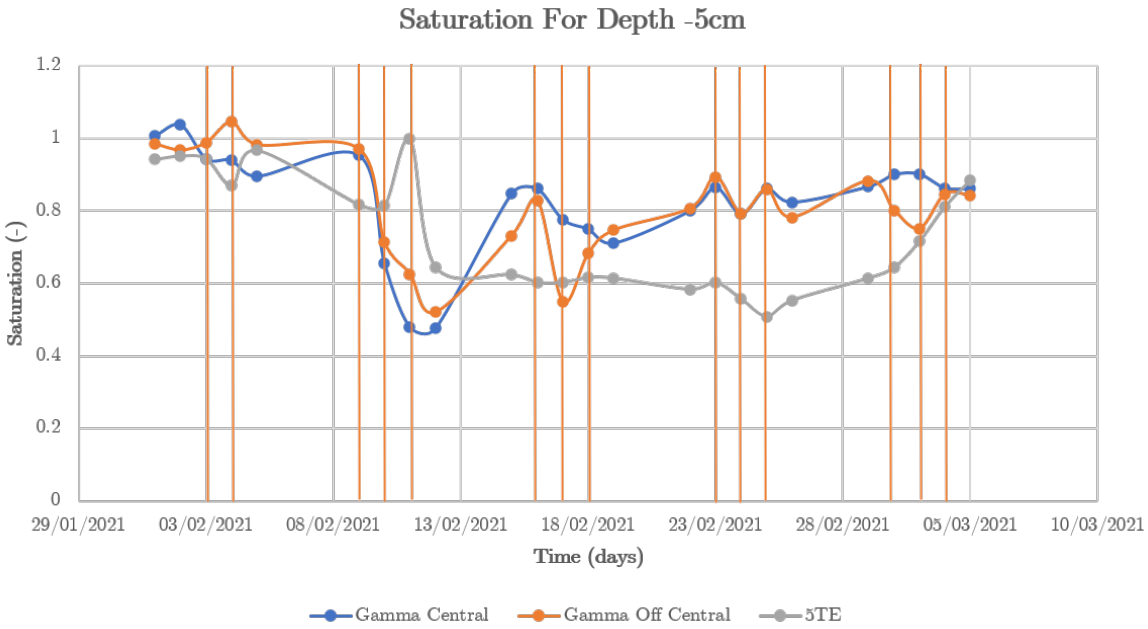


Figure 4.2.: The saturation behaviour over time from the 5TE sensor (grey), gamma central (blue) and gamma off central (orange) data at depth -5cm. Vertical orange lines convey the days when the nutrients were added.

### 4.1.3. Depth -20cm

The 5TE sensor data (grey line) showed that the saturation remained close to full saturation throughout time at depth -20cm (Figure 4.3). However, the gamma data told a different story as it fluctuates throughout. For the gamma central data (blue line), the saturation went above 1 a couple of times, specifically on 16/02, 18/02, 21/02, and 01/03 onward. Nevertheless, it remained close to full saturation, except on 03/02 where there was a drop in saturation. The saturation for the gamma off-central data (orange line) showed mostly unsaturated conditions throughout time but only increased close to full saturation on 05/03. In both the central and off central data, there was a significant drop in the saturation on 17/02, which went against the pattern it was following. Again, the expectation was that the saturation would remain close to full saturation throughout the experiment, which the 5TE data has shown and the gamma central data to an extent; however, the gamma off central data show periods of unsaturated conditions.

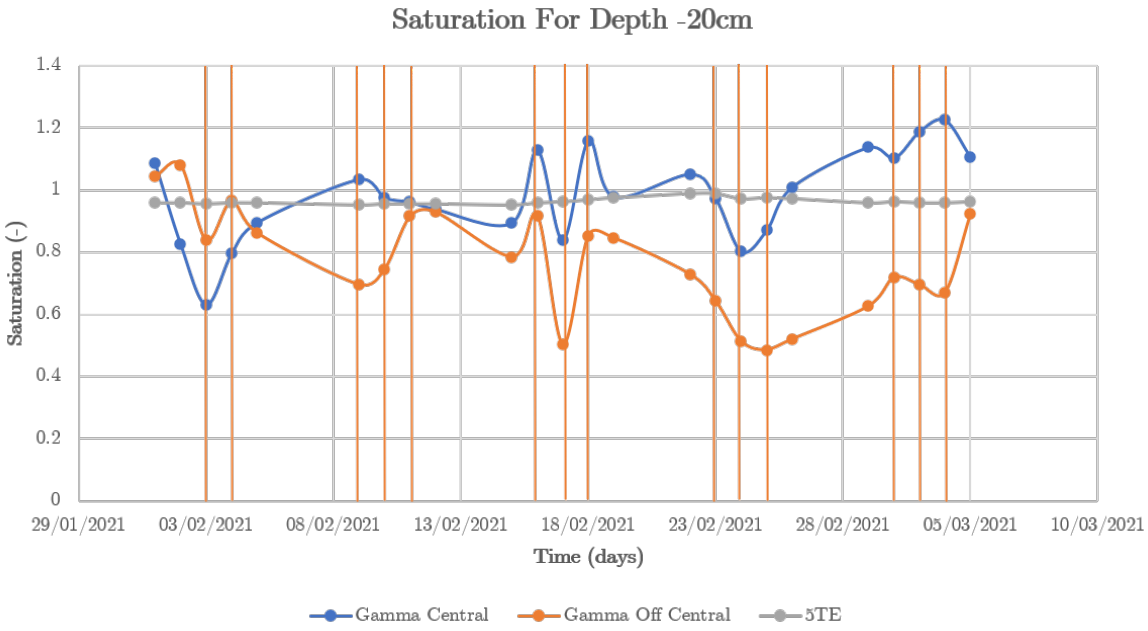


Figure 4.3.: The saturation behaviour over time from the 5TE sensor (grey), gamma central (blue) and gamma off central (orange) data at depth -20cm. Vertical orange lines convey the days when the nutrients were added.

### 4.1.4. Depth -35cm

The saturation from both the gamma and the 5TE sensor remained relatively close to full saturation until 16/02 (Figure 4.4). After 16/02, the saturation on the 5TE slowly decreased and remained unsaturated. For both the gamma data, the saturation increased, then decreased, then significantly increased above 1. There was a sudden drop in the saturation on 17/02 for both gamma data, similarly seen in the depth -20cm data (Figure 4.3), which went against the pattern it was trying to follow. This could be an anomaly in the gamma intensity reading on that day. Full saturation was anticipated in all of the data, which both gamma data have shown to an extent - but the 5TE indicated the opposite.

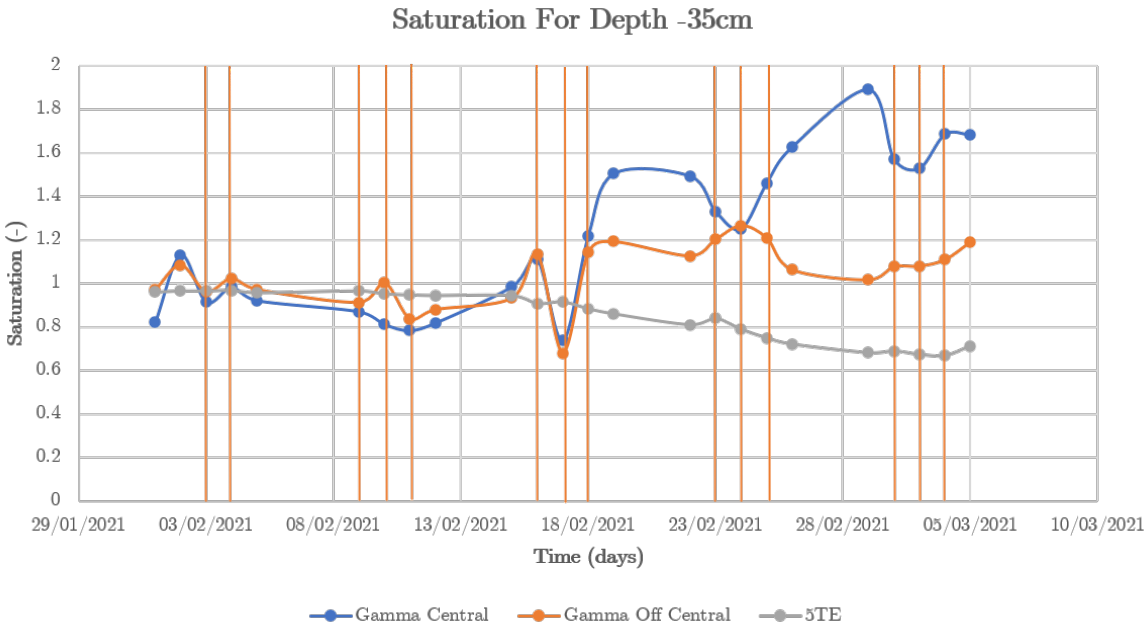


Figure 4.4.: The saturation behaviour over time from the 5TE sensor (grey), gamma central (blue) and gamma off central (orange) data at depth -35cm. Vertical orange lines convey the days when the nutrients were added.

### 4.1.5. Depth -46.5cm

The gamma data shows a fluctuation in saturation throughout time, while the saturation for the 5TE (grey line) remained constant as it was further away from the leaking hole (Figure 4.5). From 22/02 onward, the saturation was above 1 for the gamma off central data (orange line) and started to decrease below 1 after 02/03. The saturation also went above 1 for the gamma central data (blue line) on 05/03.

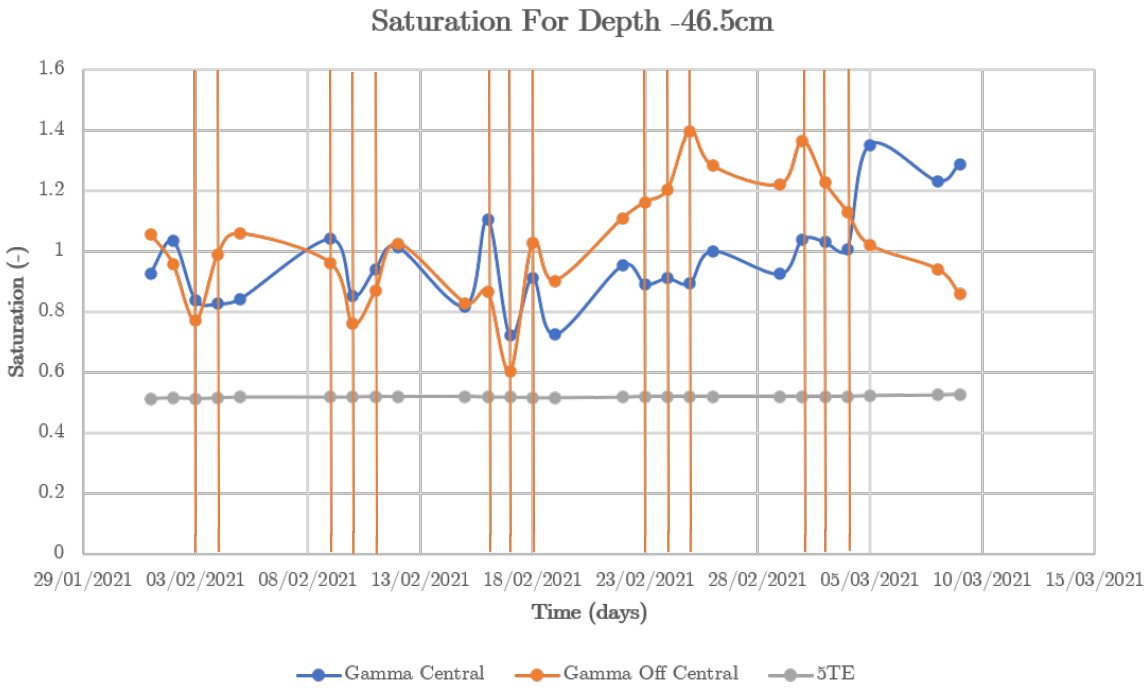


Figure 4.5.: The saturation behaviour over time from the 5TE sensor (grey), gamma central (blue) and gamma off central (orange) data at depth -46.5cm. Vertical orange lines convey the days when the nutrients were added.

## 4.2. Sub-Question 2: Seepage Flow Rate

Figure 4.6 below illustrates the decline in the effluent flow rate over time. Orange lines represent when nutrients were injected and the green line highlights when the nutrients reached depth -35cm (near the fractured plate), which is on 06/02 based on the ECb data (see Appendix C.3.1). From 01/02 until 09/02, the bottom effluent flow rate was relatively the same at about 1.9 ml/hr except on 02/02. The effluent flow rate then decreased from 10/02 onward. From 15/02 until 19/02, the effluent decreased in a fluctuating manner. After 23/03, the effluent stayed relatively the same, around 0.19 ml/hr. The effectiveness of BioSealing on the decline in flow is shown in Figure 4.7.

The clogging factor increases almost exponentially from a factor of 1 to a factor of 15-16 for all depth intervals. After that, they stabilized around a factor of 11. It was anticipated that at depth interval -35cm to -46.5cm (yellow line) would have the largest increase in clogging factor as that is where BioSealing would occur the most. However, all the depth intervals show an almost equal increase.

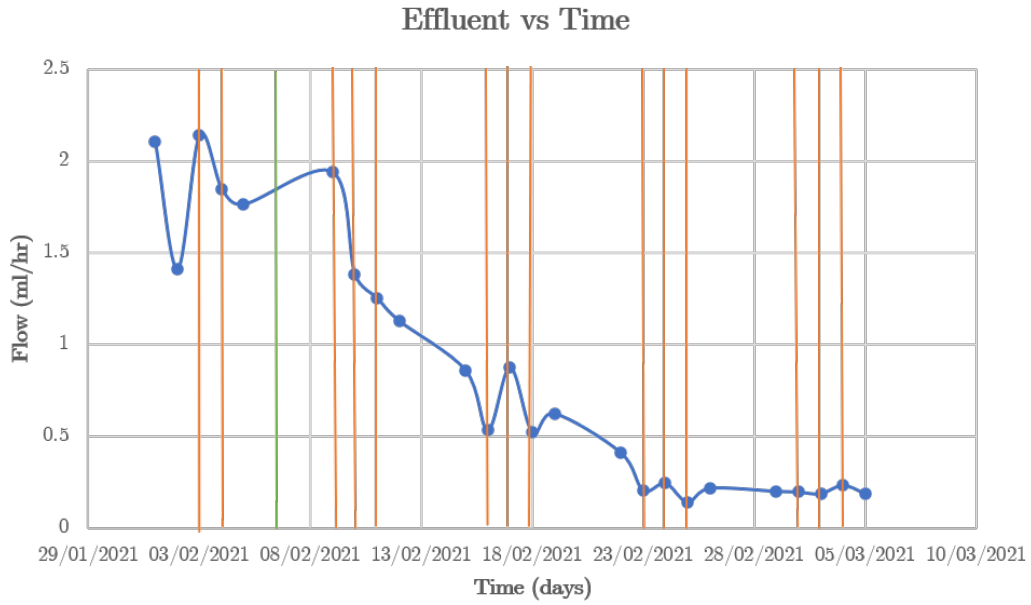


Figure 4.6.: The decline in effluent flow rate over time. Vertical orange lines convey the days when the nutrients were added and the vertical green line indicates when the nutrients reached depth -35cm

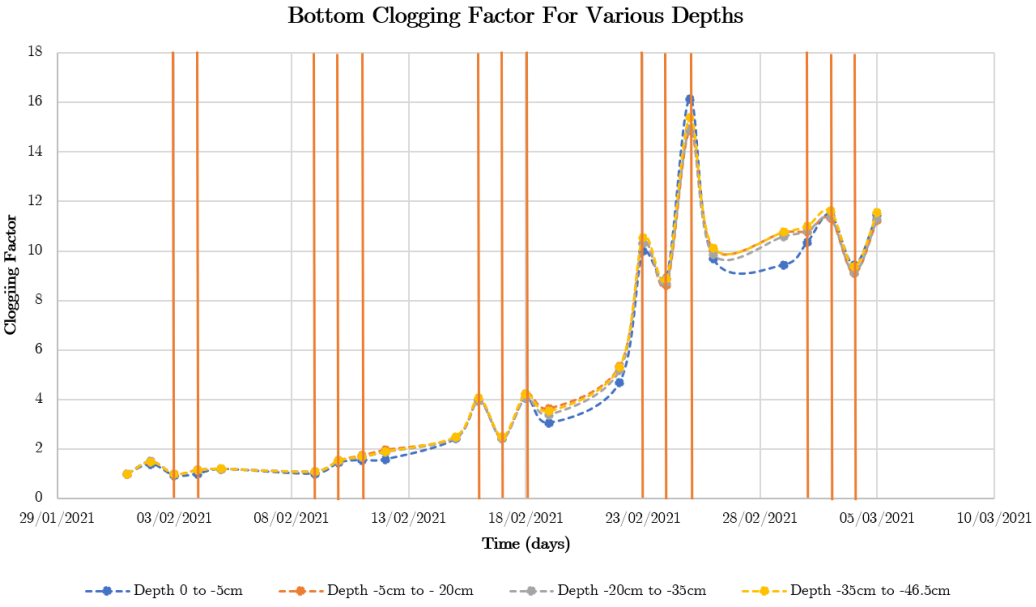


Figure 4.7.: The increasing nature of the clogging factor over time at different depth intervals: (Blue) 0cm to -5cm, (Orange) -5cm to -20cm, (Grey) -20cm to -35cm and (Yellow) -35cm to -46.5cm. Vertical orange lines convey the days when the nutrients were added.

## 4.3. Sub-Question 3: Areas of BioSealing

The total amount of 16S rRNA genes per cell is illustrated in Figure 4.8, where each distinct color represents the layer depth it was sampled from (see Figure 3.4 for the sampling locations). There were two cells, cells 3.4 and 6.1, that recorded the highest amount of genes; however, the standard error for both was also very high. The next two highest gene counts came from cells 1.3 and 5.2 with 2.84E11 and 2.30E11 genes. This means that this is where BioSealing took place the most. Depth interval 0 to -8cm (blue) would have the largest range gene count from 1.63E11 to 2.84E11 if cells 3.4 and 6.1 were disregarded. The lowest ranges were from the depth interval -52 to -57cm (grey).

When examining the gene count in terms of its total and average per layer (Figure 4.9) rather than per cell, a ranking of how much BioSealing occurred per layer can be derived. For the total gene count per layer (solid colour bars), the ranking from most BioSealing to least is: (1) 0 to -8cm [blue], (2) -32 to -40cm [yellow], (3) -24 to -32cm [orange], (4) -8 to -16cm [green], (5) -16 to -24cm [red], (6) -52 to -57cm [grey]. The average gene count (black line) ranking follows the same pattern, except for layers -8 to -16cm and -24 to -32cm where their ranks are swapped. Depth 0 to -8cm has a significantly larger gene count than the rest of the layers, indicating that this is where the most BioSealing activity is happening.

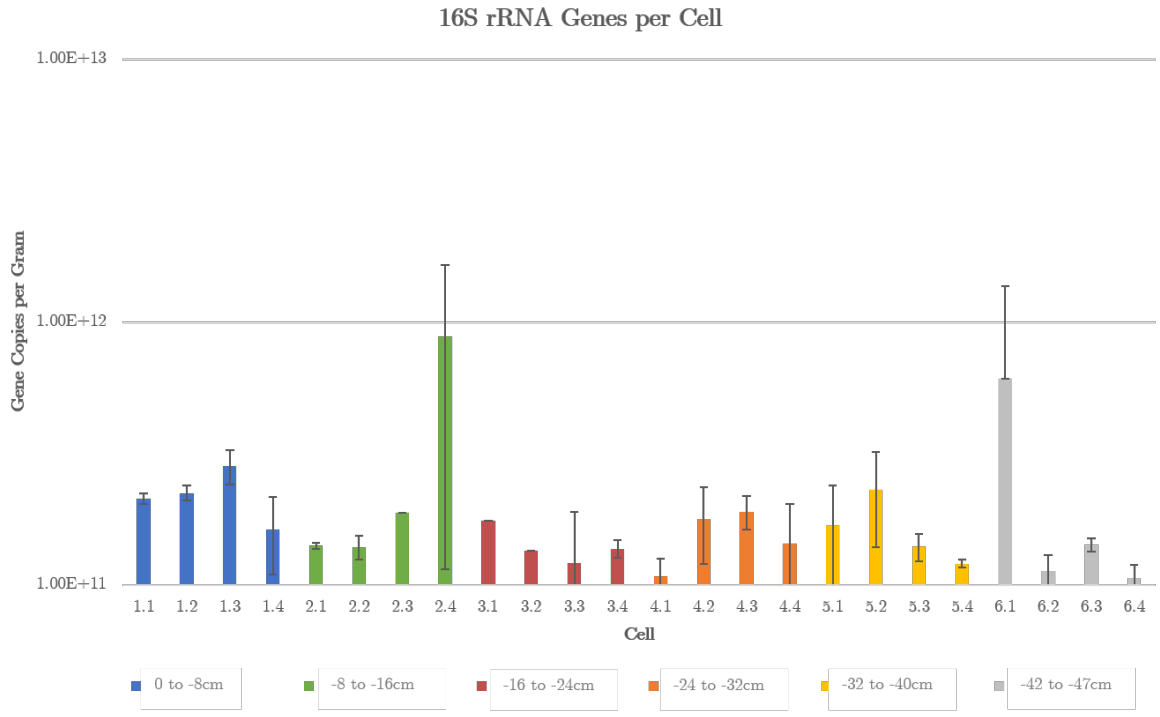


Figure 4.8.: Total 16S rRNA genes per cell with depth intervals: (Blue) 0 to -8cm, (Green) -8 to -16cm, (Red) -16 to -24cm, (Orange) -24 to -32cm, (Yellow) -32 to 40cm and (Grey) -52 to -57cm.

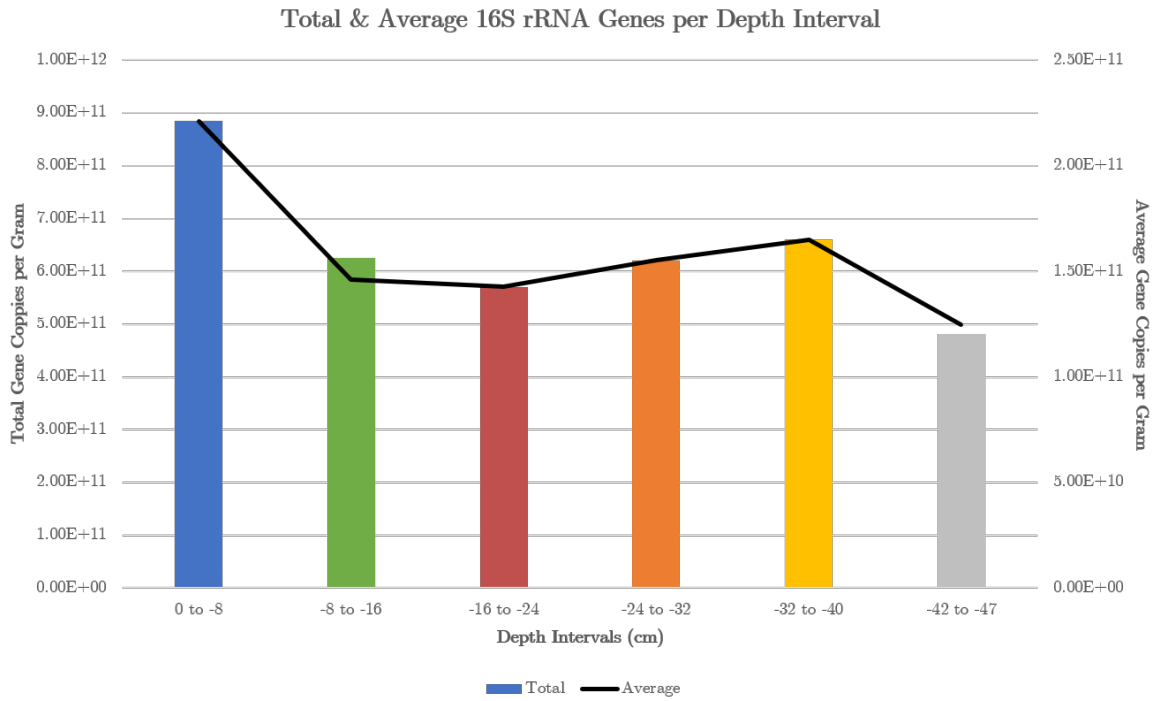


Figure 4.9.: Average 16S rRNA genes per layer (black line) and total 16S rRNA genes per layer with depth intervals: (Blue) 0 to -8cm, (Green) -8 to -16cm, (Red) -16 to -24cm, (Orange) -24 to -32cm, (Yellow) -32 to 40cm and (Grey) -52 to -57cm.

# 5. Discussion

The aim of this study was to investigate the effectiveness of the BioSealing technique in sealing a single hole fractured rock to establish a groundwater table in the overlying soil. The results indicate that it was not possible to see a rise in the groundwater table due to BioSealing because the tank became fully saturated before injecting the nutrients. Even though the tank was fully saturated, the saturation fluctuated at different locations once the nutrients entered the system. A decline in seepage flow rate was seen after some time since the first injection of the nutrients; however, the extent to which BioSealing caused this in the right area (surrounding area of the leak) is questionable as most of the activity occurred just below the soil surface. This chapter explores why these results transpired, the limitations of this study, and further recommendations.

## 5.1. Fluctuating Saturations

Before adding the nutrients, the tank was fully saturated at all depths and at the different measured locations of the gamma system and 5TE sensors. After some injections of nutrients, the saturation at all measured locations (except for the 5TE sensors at depths -20cm and -46.5cm) fluctuated throughout time, when it was expected that it would remain at full saturation at a constant value. For example, in Figure 4.2, the saturation for depth -5cm became more unsaturated in general. Interestingly, the saturation from the gamma data at depths -20, -35, and -46.5cm went beyond a saturation of 1, which is not possible as that is the maximum. The saturation at each measured location per depth behaved independently off each other as it followed their pattern, especially at depth -20cm (Figure 4.3). At this depth, the saturation either remained constant at maximum saturation (5TE sensor), went beyond maximum (gamma central), or fluctuated in unsaturated conditions (gamma off central). This signifies that these effects are primarily local events. What caused these saturation changes is the BioSealing process outlined in section 2.1.1.

When the saturation in the gamma data was above the maximum, there is more material present at that location, causing the gamma-ray intensities to be more attenuated. If the material were water, the saturation would never go beyond 1. So the material that is causing this were the soil fines created from steps 1 and 2 of the BioSealing process, where the higher acidity of the environment due to the bacterial fermentation of the nutrients caused weathering of fines. The formed EPS may have also trapped these fines in step 4. However, step 5 of BioSealing could have also caused more soil material to be at the measured locations as the nutrients can initiate small clay particle flocculation.

The decrease in saturation might suggest less water entering the tank and that water

is being drained, resulting in unsaturated conditions. This was not the case because the tank was fully saturated and the effluent flow rate is not fast enough to drain the water. Based on the BioSealing process, a more plausible explanation is that the decrease in saturation could be caused by the presence of entrapped gas byproducts from the bacterial fermentation of nutrients such as carbon dioxide and methane (Figure 5.1). This was qualitatively proven as gas bubbles were seen at the soil surface, as well as the stench that was smelt. Another reason why there was a decrease in saturation could be that preferential flow paths were formed due to BioSealing, so water is being diverted away from the measured locations, just like in the study of Seki, Thullner, Hanada, and Miyazaki (2006) (Figure 5.2). These explanations are mostly accurate for the gamma data but not for the 5TE sensors to an extent.

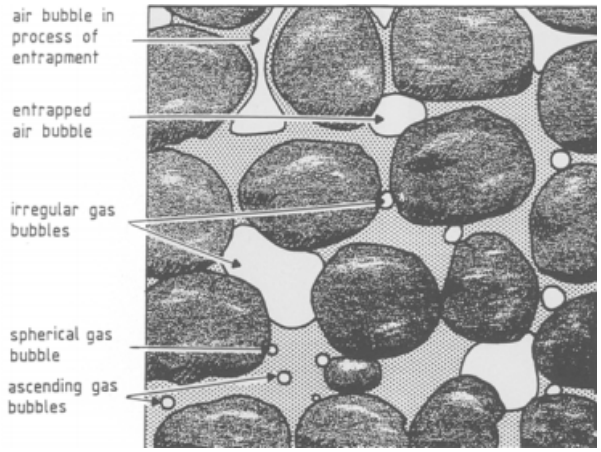


Figure 5.1.: Schematic depiction of gas byproducts from bacterial fermentation entrapped within a porous media as air bubbles (Ronen et al., 1989).

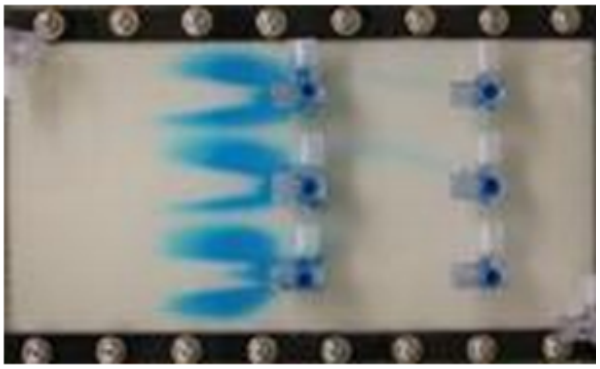

Figure 5.2.: Bioclogging influencing preferential flow paths (dyed in blue) (Seki et al., 2006).

In Figure 4.4, the gamma data shows that the saturation increased above the maximum, which means that there is more fine material present at this depth. As the saturation increases in the gamma data, the saturation decreases in the 5TE data. What is causing this decrease may not be the presence of gas or preferential flow paths but that the

accumulation of fines at this depth causes the porosity to decrease. This implies less pore space available for water to fill, resulting in a decrease in saturation. This is reflected in the ECb data, where the ECb dropped below the initial value when it was at full saturation and remained that way throughout the experiment (see Appendix C.3.2). The time that these events occurred coincides with each other around 18/02. These reasons for the decrease in saturation for the 5TE sensors cannot be applied to the decrease seen at depth -5cm (Figure 4.2) because the ECb mostly remained above the initial value (Appendix C.1). Thus, this decrease is likely due to gas.

The changes in saturation from both the gamma and 5TE data are quite complex to describe as it was difficult to attribute the mechanisms behind the patterns that were seen. Rockhold et al. (2005) experienced similar issues when investigating bioclogging in unsaturated conditions - using TDR to measure the saturation. They attributed the changes in saturation from the following mechanisms: (1) biofilms or cell aggregates clogging pore throats, (2) the production of carbon dioxide gas and occlusion, (3) the generation of biosurfactants such as excess fatty acid production, along with its accompanying decrease of gas-liquid interfacial tension, (4) the coating of soil by biofilms causing the wettability of the soil to change, and (5) a combination of these mechanisms. The factors described that contributed to the fluctuating saturations in this study further confirms the observations seen by Rockhold et al. (2005). Another mechanism that they did not mention but in other biolcogging and BioSealing literature such as Mostafa and Van Geel (2012) and Blauw et al. (2009), respectively, is the involvement of fines in the clogging process.

## 5.2. Decline in Flow Rate

The initial effluent flow rate was low at 1.9 ml/hr and it was predicted that it would be higher. It is believed that what caused this to happen was the leaking hole constricting the flow through it (further explained in 5.4.1). Nevertheless, after about a week since the first injection of nutrients, there was a noticeable decline in the effluent flow rate. The nature of the decline seemed to be of an exponential decrease to an extent and then it plateaued after about a month since the first nutrient injection (Figure 4.6). This result provides further evidence on the theory that the flow rate declines exponentially due to bioclogging, as explored in section 2.1.3. Specifically, it only exhibits the last two of the four phases of the decline seen from the bioclogging literature review of Baveye et al. (1998) (Figure 2.1). This illustrates that some form of BioSealing has taken place. Its effectiveness by a clogging factor of 11 further confirms this.

The increase in clogging factor over time seemed to be exponential as well (Figure 4.7), which further confirms the results presented in the research of Veenbergen et al. (2005) and Liao et al. (2007) that effective BioSealing increases exponentially. Despite this, the results of this experiment do not fit with the notion that BioSealing mostly occurs near the surrounding area of the leak because there seems to be equal clogging across all depths (Figure 4.7). The research of Veenbergen et al. (2005) and Liao et al. (2007) have illustrated that the clogging factor near the leak increased exponentially at a

larger magnitude than at other depths and this was not seen in this experiment.

A plausible explanation for this could be that since the effluent flow rate was low to being with, the pressure head located below the leakage hole plate (depth -46.5cm) was already at its minimum. If the effluent flow rate were higher at the start, the pressure head at depth -46.5cm would be higher and it would then decrease to its minimum, which means a larger pressure head difference from t=0 to t=t. A larger pressure head difference would then result in a higher clogging factor based on equation (2.6). This poses the question of whether BioSealing did occur across all depths equally or that using the clogging factor analysis to determine the location of effective clogging is not viable for this experiment. A bacterial count analysis was then done to have a better understanding if BioSealing transpired equally at all depths or not.

## 5.3. BioSealing in the Right Areas?

The only cell that has shown to have a relatively high amount of BioSealing in the surrounding area of the leak is cell 5.2 (Figure 4.8). It was anticipated that cell 5.3 would have lots of biological activity also as it is in the surrounding area, but that was not the case. In reality, most of the clogging occurred near the soil surface (depth interval 0 to -8cm). This was proven further in the average and total gene count per layer as layer 0 to -8cm was the largest (Figure 4.9). This suggests that most of the injected nutrients hung around this depth and only a few traveled further down. Determining the retardation factor (R) and the adsorption coefficient ($K_d$) for the nutrients with this type of soil revealed that this was the case as R=6.4 and $K_d$=1.51 $cm^3/g$, which is relatively high (see Appendix C.3.1 for the calculations). In bioclogging literature, it was expected that there would be more clogging happening at depths near the inlet than at other depths based on their results (Fuchs, Hahn, Roddewig, Schwarz, & Turković, 2004; Mostafa & Van Geel, 2012; Rockhold et al., 2005; Seifert & Engesgaard, 2007; Seki et al., 2002; Zhong & Wu, 2013a; Zhong et al., 2013b).

In the research of Zhong and Wu (2013a) and Zhong et al. (2013b), they investigated bioclogging under saturated conditions using a constant head method from a bottom-up approach without a leaking hole plate. Their results illustrate that clogging happened mostly at depths near the inlet than at depths near the outlet. In addition, clogging was higher near the outlet than in the middle of their column. So the order of effective clogging is: (1) near the inlet, (2) near the outlet, and (3) middle. To an extent, their order of effective clogging resembles what was discovered in section 4.3, where BioSealing mostly happened near the soil surface than near the depths of the leakage hole and the lowest found in the middle layers of the tank.

In BioSealing literature, their experiments were done from a bottom-up approach using a constant head method as well and have proven that clogging happened primarily in the surrounding area of the fracture than at the inlet (Liao et al., 2007; Veenbergen et al., 2005). The only difference between the bioclogging and BioSealing experiments is the presence of the leaking hole plate. This implies that the existence of the leaking hole supports the BioSealing Process step 3 in section 2.1.1. In theory, this research should

follow the results of the BioSealing literature, but that was not the case. It is speculated that these differences in results emerged because of the differences in the initial flow rate of the soil system.

In both bioclogging and BioSealing literature, their hydraulic conductivities and the measured outflow in their experiments, respectively, are significantly larger than this research. For example, the hydraulic conductivity in the experiment of Zhong and Wu (2013a) is around 69 m/d and the initial outflow in the study of Liao et al. (2007) is 15 l/d. Compared to this research, the hydraulic conductivity is 0.4536 m/d and the initial outflow is 0.048 l/d, which is significantly lower. This signifies that physical factors, in this case, the flow rate through the system, play an essential role in the bioclogging process.

The bioclogging literature review of Thullner (2010) confirmed that the role of flow rate does influence the bioclogging process. They discussed that higher flow rates could lead to higher concentrations of biomass in downstream areas due to the redeposition of biomass from upstream areas caused by shear forces and sloughing (Figure 5.3). In addition, higher flow rates allow higher concentrations of nutrients to reach the downstream areas as well. The latter is what BioSealing Process step 3 (section 2.1.1) tried to explain, but the BioSealing literature review of Blauw et al. (2009) and Van Paassen (2011) did not mention that the redeposition of biomass from upstream to downstream areas due to higher fluxes could also play a role in the sealing of a fracture. In addition, the BioSealing research of Veenbergen et al. (2005) even claimed that the clogging would happen near the leak independently of the flow speed, which is not the case for this experiment.

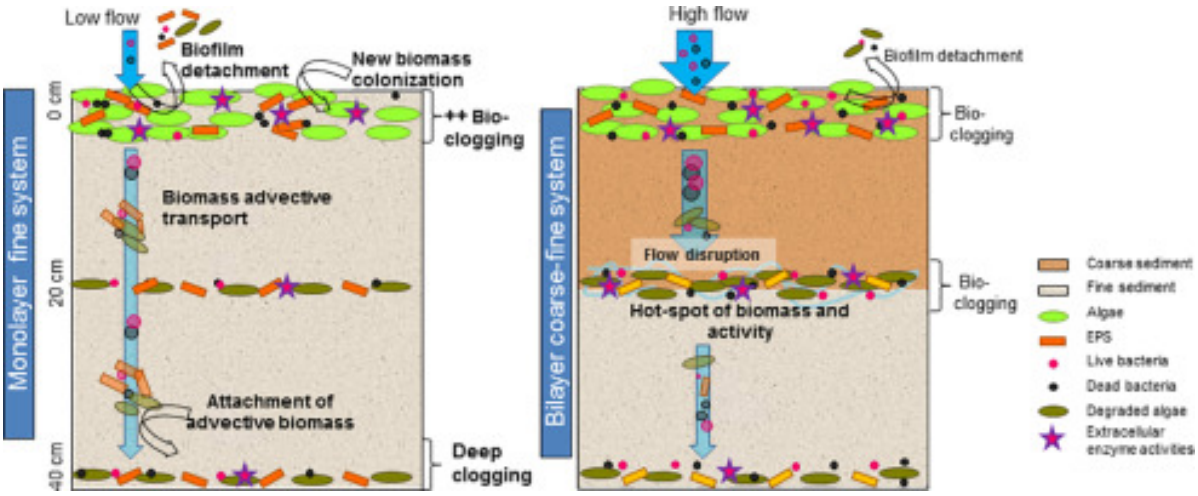


Figure 5.3.: Schematic representation of flow rate influence on biomass redepostion (Perujo et al., 2019).

## 5.4. Limitations

### 5.4.1. Saturated Tank

In section 4.1.1, the results had shown that a water table was rising within the tank and a pool of water developed on top of the soil surface before any nutrients were added. It was expected that an unsaturated steady-state flow system would be produced based on 2D modeling results during the designing phase of the experiment (Cecchetto, 2021). The main reason why this happened is due to a bottle-neck effect caused by the leaking hole as it restricted the area in which the water can flow through the leak. Consequently, the flow through the leak was slow and this is reflected in the initial effluent flow rate, which was 1.9 ml/hr. In comparison to the influent dripping rate of 120 ml/hr, the effluent rate is almost 63 times smaller, which is why the effluent flow rate was not fast enough to establish an unsaturated steady-state flow. This occurrence was not reflected in the modeling investigations, however.

The mismatch between the modeling results and reality was believed to be caused by how the 2D model interprets the nature of the leaking hole. The area of the hole could be larger than reality when translating the 2D model into 3D and this has an impact on how water flows through the leak. With a bigger area, more water can seep through to facilitate an unsaturated steady flow. In addition to this, the soil used in this experiment posed a problem.

As previously mentioned in section 3.1.2, Cecchetto (2021) reported that there was a mismatch in the $K_s$ value of the soil between the HYPROP analysis (0.017 cm/hr) and the tank system (1.80 cm/hr). The $K_s$ was significantly slower than what was observed in the tank. With this in mind, there may be heterogeneity in hydraulic conductivity within the tank, where the $K_s$ is smaller in the leaking hole than in other regions. This results in a slower flow rate through the leak, which led to the full saturation of the tank.

Observing the establishment of a groundwater table due to BioSealing the leaking hole was no longer possible as the tank became fully saturated and this hindered in answering the research question of this study. However, this limitation can still indirectly answer the research question to a small extent. In theory, if the leaking hole were larger, more water would permeate through and the overlying soil would not hold as much water, i.e., a small groundwater table is produced. Reducing the size of the hole would allow less water to flow through it and the overlying soil would hold more water to produce a larger groundwater table. In principle, the reduction in the size of the hole indirectly reflects the BioSealing technique. It could be the case that for the type of soil used in the experiment, combined with the small size of the leakage hole acting as effective BioSealing, the experiment did establish a groundwater table.

### 5.4.2. Influences on the Flow Decline

The results of this experiment cannot confirm whether the decline in the effluent was solely due to clogging because other factors may influence it as well. For example, step 5 of the BioSealing process (section 2.1.1) states that the injected nutrients can initiate

small clay flocculation and this can clog up the pores so that less water can flow through it (Blauw et al., 2009; Van Paassen, 2011). In addition, air bubbles from gas byproducts can reduce the flow rate, according to Ronen et al. (1989). These identified factors interfere with answering the central research question when investigating the effectiveness of the BioSealing technique. However, it can be argued that these factors are all part of the BioSealing principles, so overall, these factors combined can result in effective clogging.

### 5.4.3. Validity of the Saturation Measurements

As discussed in section 5.1, it was difficult to attribute precisely which mechanisms due to BioSealing correspond to a particular change in the saturation. This has an impact on the validity of the methods used to measure saturation. For instance, when examining the gamma data, it is difficult to know whether the increase in saturation is due to more water being present in the measured location or it was due to more soil material. The same can be said for the decrease in saturation as it could be due to preferential flow paths or air bubbles. The 5TE sensors are prone to this as well, but to a lesser extent because the ECb data can help distinguish between the different mechanisms behind the saturation changes. Since the gamma and 5TE sensors were measured at different locations, they record local events, which means that the saturation measurements cannot be compared. Nevertheless, as long as the mechanisms are kept in mind, the methods used to measure the saturation in this experiment are still helpful to indicate the activity inside the tank.

## 5.5. Recommendations

### 5.5.1. Experimental Design Improvements

Further research is still needed to answer the central research question as this study could not fully address it due to the unexpected saturated tank outcome. To improve upon this, it is recommended to use porous media such as clean sand as that has a higher hydraulic conductivity to reduce the bottle-neck effect at the leakage hole. This allows water to permeate through the hole faster, which would help establish an unsaturated steady-state flow. In addition to that, it would help with transporting more nutrients towards the hole so that more biomass can be formed in the correct area. Future studies should consider that if clean sand is used, inoculation of microorganisms in the sand is required to help promote biomass generation.

If an unsaturated steady-state flow still cannot be established, future research should consider increasing the area of the leakage hole. There is a concern that increasing the hole area too much would hinder the BioSealing process; however, the field study of Veenbergen et al. (2005) has shown that it is possible to seal a leak that has a diameter of 8cm.

The injection method could be better if it were to change from the dripping system to

directly inserting tubes into the soil. This avoids the flux through the soil system being partly defined by the infiltration rate and more defined by the pump flow rate. The pump flow rate could be higher also to encourage more nutrients to be flown towards the leak and encourage the redeposition of biomass towards downstream areas. However, a balance must be found between having higher flow rates and establishing an unsaturated steady-state flow; otherwise, a saturated flow is produced.

To make the experiment a more accurate representation of the conditions in dryland regions such as Yunnan, future experiments are encouraged to use the soil from those dryland regions. That would require collecting and delivering the soil across different countries, which may be inconvenient unless the experiment is done in that country. Future studies could also consider creating a more accurate representation of the fractured bedrock. This would demand an additional study on the nature of the fractured bedrock in that specific dryland region. For instance, the nature of a fractured bedrock can be categorized into three types: (1) purely fractured medium, (2) double porosity medium, and (3) heterogeneous medium (Singhal & Gupta, 2010) (Figure 5.4). Water would then flow differently based on the fracture type; for example, in a purely fractured medium, the flow of water would be based on the parallel plate model.

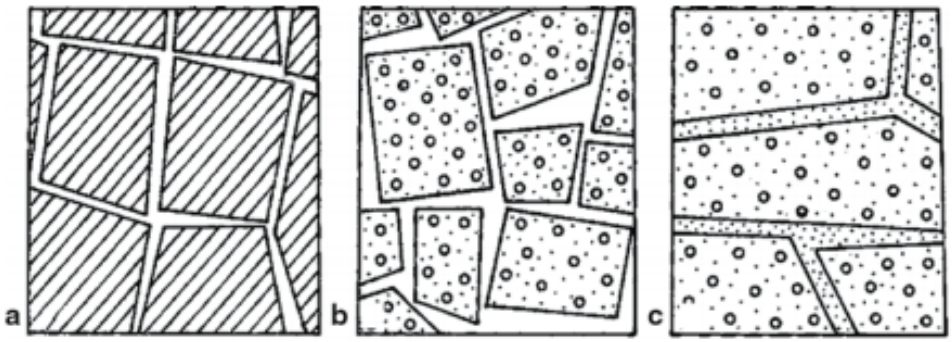


Figure 5.4.: Schematic depiction of fractured rock formations (Singhal & Gupta, 2010). (a) A purely fractured medium where the permeability and porosity is mainly defined by the interconnected fractures that exist between impervious blocks. (b) The double porosity medium consists of matrix blocks and fractures. Both facilitate water flow but it is mainly from the fractures. (c) A heterogeneous medium is defined by silty or clay material filling the fractures. This results in having a substantially reduced permeability.

### 5.5.2. Modelling Approach

Further research could investigate the research question from a modeling approach instead of an experimental route. Modelling BioSealing in unsaturated media would need to consider a variety of factors to define mathematically. These factors can be categorized into four groups: (1) solute transport, (2) microbial growth, (3) bioclogging, and (4) water flow (Thullner, 2010). Each of these groups influences the other, as shown in Figure 5.5. In solute transport, equations are needed to define the transport of nutrients and

biomass, including detachment and attachment. For microbial growth, future studies need to consider the (bio)reactive transformation from nutrients and microorganisms to biomass. A decision also needs to be made on how the biomass accumulates, whether in flocs, aggregates, or both. The common way to mathematically characterize bioclogging is the reduction of hydraulic conductivity in relation to biological growth in pores, such as equation (2.5) in section 2.1.2. That way, the mobile and immobile (biomass porosity) domains are considered. The change in hydraulic conductivity would then affect the water flow in an unsaturated porous medium, which can be derived using Darcy's law and the continuity equation.

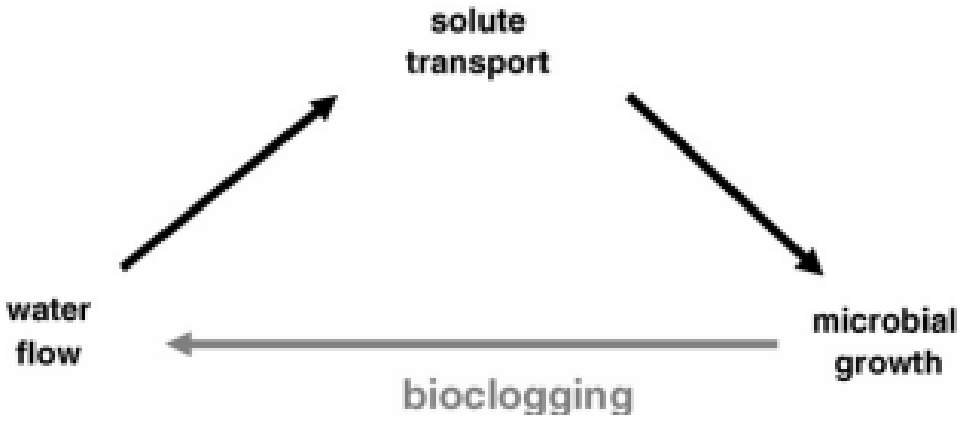


Figure 5.5.: Schematic depiction of the relationships between the four groups: (1) solute transport, (2) microbial growth, (3) bioclogging and (4) water flow (Thullner, 2010).

### 5.5.3. Beyond The Scope: Land Restoration

If lab and field experiments successfully prove that the BioSealing technique is effective in sealing fractures to establish a groundwater table, further research could investigate the ecological impact this has in dryland regions. This goes beyond the scope of this study, where the original focus was on the variables highlighted in red in Figure 2.3b, but it is now shifted to the variables in green (Figure 5.6). There is the potential that establishing a groundwater table can help restore the land in dryland regions.

In ecology, the effect that BioSealing has on its environment can be perceived as what ecosystem engineers do to an extent. They modulate the availability of resources directly or indirectly for other organisms by altering the physical state of biotic or abiotic materials (Jones, Lawton, & Shachak, 1994). As a result, they can maintain, modify and create habitats. This modification to the environment needs to be studied before restoring degraded land because some degraded land is resilient to restoration efforts. It is recommended to use the Alternative Stable State model from the research of Suding, Gross, and Houseman (2004) to study this as it considers system thresholds and feedbacks to help identify, prioritize and address specific constraints in land restoration.

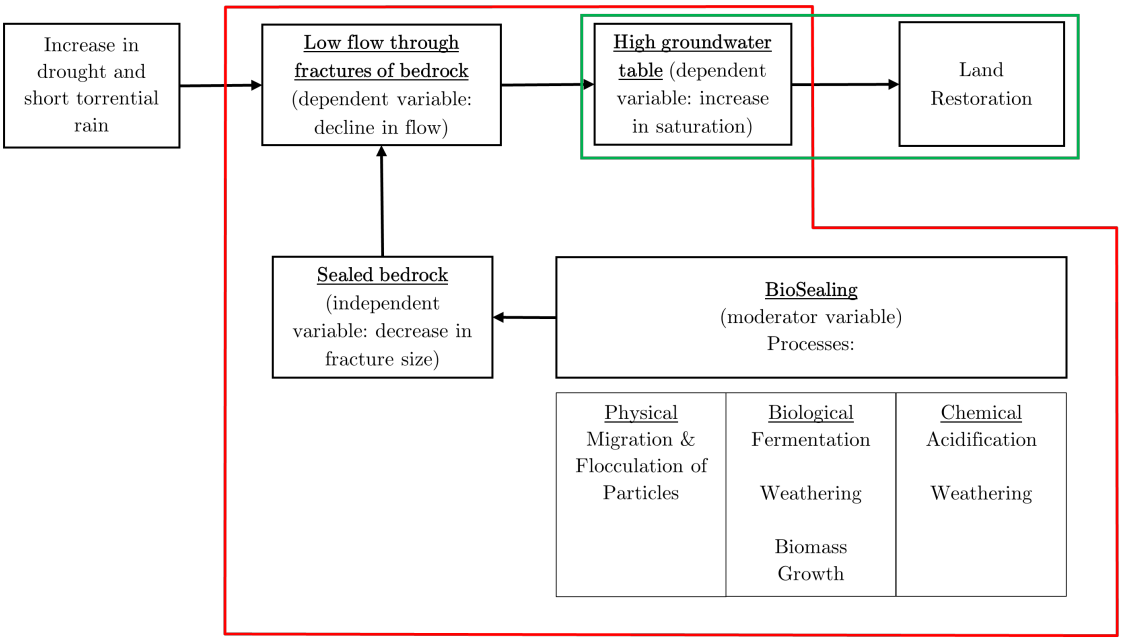


Figure 5.6.: New area of focus beyond the scope of this study highlighted in green.

# 6. Conclusion

The research question of this study was, "To what extent is the BioSealing technique effective in sealing a single hole fractured rock to establish a groundwater table in the overlying soil?". Based on the experimental results from the saturation, flow, and bacterial count measurements, this research cannot fully address the question due to the unexpected saturated tank outcome. Because of this, it was no longer possible to observe a groundwater table being established.

Despite this obstacle, it was still feasible to address the effectiveness of the BioSealing technique in sealing the fracture but under saturated conditions rather than the intended unsaturated conditions. The effluent flow rate results have shown that due to the injection of the nutrients and subsequently BioSealing, the flow rate declined exponentially with a clogging factor of 11. This indicates that the technique effectively slows down the flow rate, but it remains to be seen whether BioSealing took place in the surrounding area of the leakage hole.

The bacterial count analysis revealed that there was some BioSealing involved in the leakage hole area, but most of the biomass growth activity happened near the soil surface. It follows that the single hole fracture was sealed to a small extent; however, the sealing nature is questionable because it is believed that biomass is not the sole contributor to the flow decline. Analysis from the gamma and 5TE sensor data conveyed that air bubbles from gas byproducts of bacterial fermentation and small clay flocculation from the nutrients could have played a role in decreasing the effluent flow rate. It can be argued that these two additional factors are all part of the BioSealing principles, making the overall technique effective.

The expected outcome for this research was observing high amounts of biomass in the surrounding area of the leakage hole. As the area for water to pass through the hole becomes smaller due to biomass accumulation, a groundwater table would be established and rise towards the soil surface. Upon reflection on the experimental setup, a couple of changes can be made to achieve the expected results. For example, replacing the soil used in the experiment with a porous media that has a higher hydraulic conductivity, such as sand, would facilitate an unsaturated steady-state flow and prevent the tank from becoming fully saturated. Combining this with increasing the injection flow rate would encourage more biomass growth and accumulation near the leakage area.

Future studies can improve this experiment even further by designing the experiment to reflect the actual conditions of dryland regions as close as possible. A modeling approach can also be done to answer the research question, but that would require defining physical, chemical, and biological processes mathematically. If lab and field studies are successful, it is useful to do an environmental impact study on BioSealing as a method to restore degraded land.

Although the research question was not fully addressed, this research still has some knowledge to contribute to the field of study. For instance, the fluctuating saturation results confirm the research of Rockhold et al. (2005) in the difficulty of interpreting the changes in saturation and attributing its corresponding mechanism. In addition, this study further proves the theory that BioSealing or bioclogging causes a decrease in flow rate and increase in clogging factor exponentially to an extent. The observation of higher clogging activity near the inlet depth than the outlet and middle depths due to low flow rates of the system in bioclogging literature was also demonstrated in this experiment.

# References


Abdel Aal, G. Z., Atekwana, E. A., & Atekwana, E. A. (2010). Effect of bioclogging in porous media on complex conductivity signatures. *Journal of Geophysical Research: Biogeosciences*, *115*(G3).

Adhikari, U., Nejadhashemi, A. P., & Woznicki, S. A. (2015). Climate change and eastern africa: a review of impact on major crops. *Food and Energy Security*, *4*(2), 110–132.

Admiraal, B., & Molendijk, W. O. (2006). Modification of soil-characteristics with biotechnology..

Andersen, L. S. (2013). *Groundwater in china* (Tech. Rep.). COWI, Parallelvej 2, 2800 Kongens Lyngby, Denmark: COWI.

Badi, L. (2018). *Solute transport in the unsaturated zone–an experimental approach* (Unpublished master's thesis). UU Dept. of Earth Sciences.

Baveye, P., Vandevivere, P., Hoyle, B. L., DeLeo, P. C., & de Lozada, D. S. (1998). Environmental impact and mechanisms of the biological clogging of saturated soils and aquifer materials. *Critical reviews in environmental science and technology*, *28*(2), 123–191.

Biekart, S. (2018). *Dispersivity-saturation relation for fine sand, collected with column experiments* (Unpublished master's thesis). UU Dept. of Earth Sciences.

Blauw, M., Lambert, J., & Latil, M.-N. (2009). Biosealing: a method for in situ sealing of leakages. In *Proceedings of the international symposium on ground improvement technologies and case histories, isgi* (Vol. 9, pp. 125–130).

Campbell, C. (2014). *Soil moisture 201: Water content measurements methods and applications.* Retrieved from `https://www.youtube.com/watch?v=jzYCuspFhwo`

Cecchetto, G. (2021). *Design and construction of an experimental setup for biosealing application in artificial groundwater recharge* (Unpublished master's thesis). UU Dept. of Earth Sciences.

Chauhan, B. S., Mahajan, G., Randhawa, R. K., Singh, H., Kang, M. S., & Kaur, P. (2014). Global warming and its possible impact on agriculture in india. In *Advances in agronomy* (Vol. 123, pp. 65–121). Elsevier.

de Jong, A. (2020). *Environmental impacts on the microbial methane cycle in freshwater sediments* (Unpublished doctoral dissertation). [Sl: sn].

Dingman, S. L. (2015). *Physical hydrology.* Waveland press.

Dontsova, K., & Norton, L. D. (1999). Effects of exchangeable ca: Mg ratio on soil clay flocculation, infiltration and erosion. In *Proceedings 10th international soil conservation organization meeting* (pp. 24–30).

Engesgaard, P., Seifert, D., & Herrera, P. (2006). Bioclogging in porous media: tracer studies. In *Riverbank filtration hydrology* (pp. 93–118). Springer.

Fuchs, S., Hahn, H. H., Roddewig, J., Schwarz, M., & Turković, R. (2004). Biodegradation and bioclogging in the unsaturated porous soil beneath sewer leaks. *Acta hydrochimica et hydrobiologica*, *32*(4-5), 277–286.

Haque, M. M., Rahman, A., & Samali, B. (2016). Evaluation of climate change impacts on rainwater harvesting. *Journal of Cleaner Production*, *137*, 60–69.

Helmreich, B., & Horn, H. (2009). Opportunities in rainwater harvesting. *Desalination*, *248*(1-3), 118–124.

Huang, J., Yu, H., Dai, A., Wei, Y., & Kang, L. (2017). Drylands face potential threat under 2 c global warming target. *Nature Climate Change*, *7*(6), 417–422.

Jones, C. G., Lawton, J. H., & Shachak, M. (1994). Organisms as ecosystem engineers. In *Ecosystem management* (pp. 130–147). Springer.

Kummu, M., Guillaume, J. H., de Moel, H., Eisner, S., Flörke, M., Porkka, M., ... Ward, P. J. (2016). The world's road to water scarcity: shortage and stress in the 20th century and pathways towards sustainability. *Scientific reports*, *6*, 38495.

Kundzewicz, Z. W., Mata, L., Arnell, N. W., Döll, P., Jimenez, B., Miller, K., ... Shiklomanov, I. (2008). The implications of projected climate change for freshwater resources and their management. *Hydrological sciences journal*, *53*(1), 3–10.

Liao, H., Zhao, K., Lambert, J., & Veenbergen, V. (2007). Experimental study on biosealing technology for seepage prevention. *age*, *1000*(3).

Madigan, M. T., Martinko, J. M., & Parker, J. (1997). *Brock biology of microorganisms* (Vol. 11). Prentice hall Upper Saddle River, NJ.

Meter Group. (2018). *5te manual* [Device Manual]. 2365 NE Hopkins Court Pullman, WA 99163.

Mostafa, M., & Van Geel, P. (2012). Validation of a relative permeability model for bioclogging in unsaturated soils. *Vadose Zone Journal*, *11*(1).

Mukherjee, S., Mishra, A., & Trenberth, K. E. (2018). Climate change and drought: a perspective on drought indices. *Current Climate Change Reports*, *4*(2), 145–163.

Okubo, T., & Matsumoto, J. (1983). Biological clogging of sand and changes of organic constituents during artificial recharge. *Water Research*, *17*(7), 813–821.

Oostrom, M., & Dane, J. (1990). Calibration and automation of a dual-energy gamma system for applications in soil science. *Calibration and automation of a dual-energy gamma system for applications in soil science.*(145).

Oostrom, M., Hofstee, C., Dane, H., & Lenhard, R. J. (1998). Single-source gamma radiation procedures for improved calibration and measurements in porous media. *Soil Science*, *163*(8), 646–656.

Perujo, N., Romaní, A. M., & Sánchez-Vila, X. (2019). A bilayer coarse-fine infiltration system minimizes bioclogging: the relevance of depth-dynamics. *Science of the total environment*, *669*, 559–569.

Qiu, J. (2010). China drought highlights future climate threats: Yunnan's worst drought for many years has been exacerbated by destruction of forest cover and a history of poor water management. *Nature*, *465*(7295), 142–144.

Ritalahti, K. M., Amos, B. K., Sung, Y., Wu, Q., Koenigsberg, S. S., & Löffler, F. E. (2006). Quantitative pcr targeting 16s rrna and reductive dehalogenase genes simul-

taneously monitors multiple dehalococcoides strains. *Applied and environmental microbiology*, *72*(4), 2765–2774.

Rockhold, M. L., Yarwood, R., Niemet, M., Bottomley, P. J., & Selker, J. S. (2005). Experimental observations and numerical modeling of coupled microbial and transport processes in variably saturated sand. *Vadose Zone Journal*, *4*(2), 407–417.

Ronen, D., Berkowitz, B., & Magaritz, M. (1989). The development and influence of gas bubbles in phreatic aquifers under natural flow conditions. *Transport in Porous Media*, *4*(3), 295–306.

Ross, N., & Bickerton, G. (2002). Application of biobarriers for groundwater containment at fractured bedrock sites. *Remediation Journal*, *12*(3), 5–21.

Ross, N., Villemur, R., Deschênes, L., & Samson, R. (2001). Clogging of a limestone fracture by stimulating groundwater microbes. *Water Research*, *35*(8), 2029–2037.

Schotting, R. (n.d.). *Towards drought-preparedness.* (Internal Document)

Seifert, D., & Engesgaard, P. (2007). Use of tracer tests to investigate changes in flow and transport properties due to bioclogging of porous media. *Journal of contaminant hydrology*, *93*(1-4), 58–71.

Seifert, D., & Engesgaard, P. (2012). Sand box experiments with bioclogging of porous media: Hydraulic conductivity reductions. *Journal of contaminant hydrology*, *136*, 1–9.

Seki, K., Suko, T., & Miyazaki, T. (2002). Bioclogging of glass beads by bacteria and fungi. In *Trans. world congr. soil sci. symposium* (pp. 1244–1).

Seki, K., Thullner, M., Hanada, J., & Miyazaki, T. (2006). Moderate bioclogging leading to preferential flow paths in biobarriers. *Groundwater Monitoring & Remediation*, *26*(3), 68–76.

Singhal, B. B. S., & Gupta, R. P. (2010). *Applied hydrogeology of fractured rocks.* Springer Science & Business Media.

Štyriaková, I., Štyriak, I., Malachovskỳ, P., Večera, Z., & Koloušek, D. (2007). Bacterial clay release and iron dissolution during the quality improvement of quartz sands. *Hydrometallurgy*, *89*(1-2), 99–106.

Suding, K. N., Gross, K. L., & Houseman, G. R. (2004). Alternative states and positive feedbacks in restoration ecology. *Trends in ecology & evolution*, *19*(1), 46–53.

Sutherland, I. W. (2001). Biofilm exopolysaccharides: a strong and sticky framework. *Microbiology*, *147*(1), 3–9.

Thullner, M. (2010). Comparison of bioclogging effects in saturated porous media within one-and two-dimensional flow systems. *Ecological Engineering*, *36*(2), 176–196.

Topp, G. C., Davis, J. L., & Annan, A. P. (1980). Electromagnetic determination of soil water content: Measurements in coaxial transmission lines. *Water resources research*, *16*(3), 574–582.

United Nations. (n.d.). *Sustainable development goals knowledge platform.* Retrieved from `https://sustainabledevelopment.un.org/sdg12`

Van Beek, V., Den Hamer, D., Lambert, J., Latil, M., & Van Der Zon, W. (2007). Biosealing, a natural sealing mechanism that locates and repairs leaks. In *Proceedings of the 1th international conference on self healing materials, noordwijk aan zee, the netherlands* (pp. 18–20).

van der Zaan, B. (2020). Personal Communication.

Van Paassen, L. (2011). Bio-mediated ground improvement: from laboratory experiment to pilot applications. In *Geo-frontiers 2011: Advances in geotechnical engineering* (pp. 4099–4108).

Veenbergen, V., Lambert, J., van der Hoek, E., van Tol, A., & Weersma, S. (2005). Biosealing: How micro-organisms become our little allies in repairing leaks in underground constructions. In *Underground space use: Analysis of the past and lessons for the future. in: Proceedings of ita-aites world tunnel congress, istanbul, turkey* (pp. 7–12).

Witte, R. d. (2017). *Dispersivity-saturation relationship for various porous media; experiments and modelling* (Unpublished master's thesis). UU Dept. of Earth Sciences.

Zhong, X., & Wu, Y. (2013a). Bioclogging in porous media under continuous-flow condition. *Environmental earth sciences*, *68*(8), 2417–2425.

Zhong, X., Wu, Y., & Xu, Z. (2013b). Bioclogging in porous media under discontinuous flow condition. *Water, Air, & Soil Pollution*, *224*(5), 1543.

Zhuang, L. (2017). *Advanced theories of water redistribution and infiltration in porous media: Experimental studies and modeling* (Unpublished doctoral dissertation). UU Dept. of Earth Sciences.

# A. Tensiometer Calibration Results

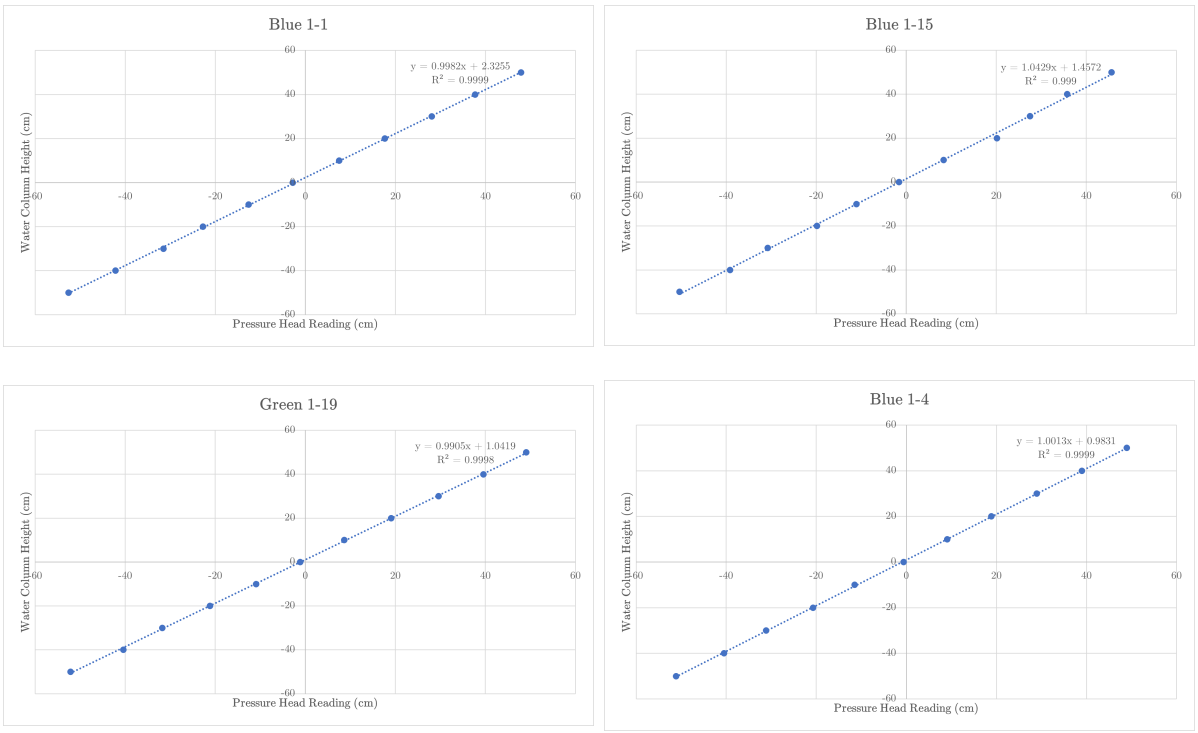


Figure A.1.: The results of the calibration of each tensiometer used during the experiment

# B. Gamma Calibration & Attenuation Results

## B.1. Compton Scattering Calibration

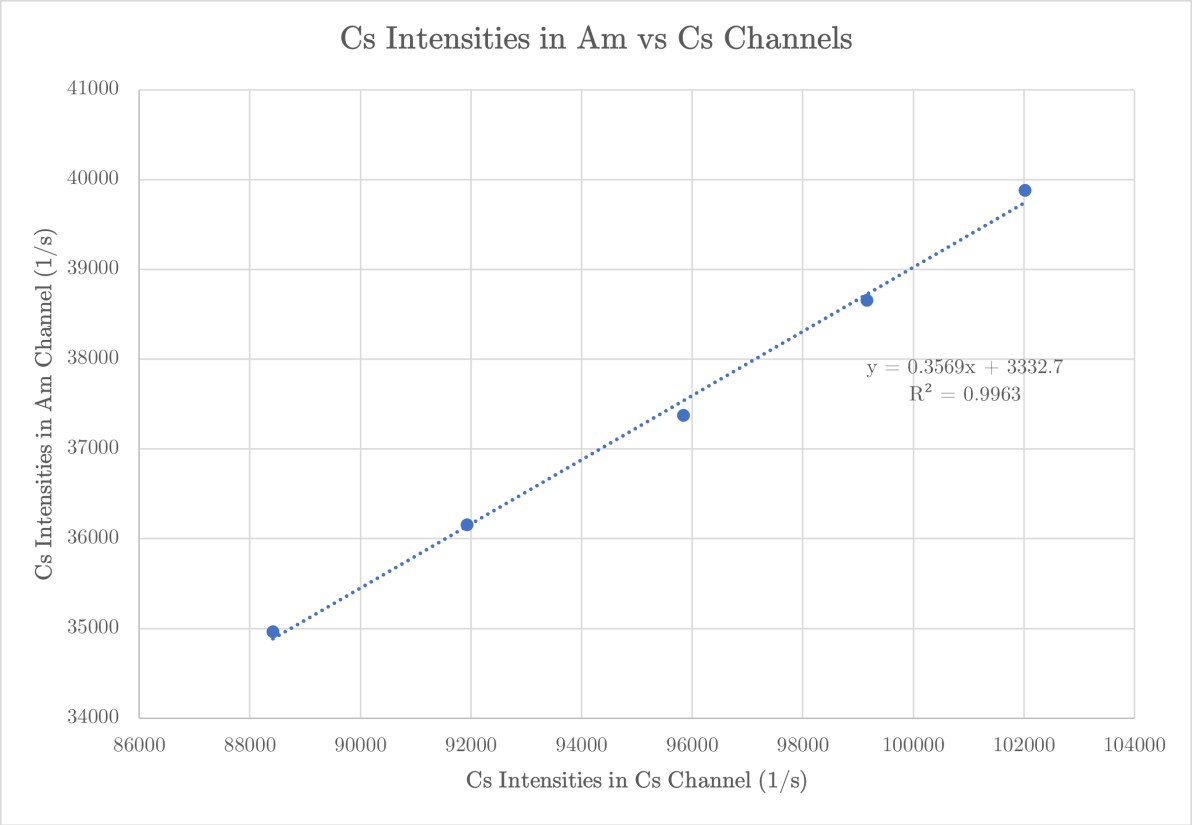


Figure B.1.: Compton scattering in the Am channel vs the Cs channel. The equation of the slope is the compton correction

# B.2. Attenuation Coefficients

## B.2.1. Water Attenuation Coefficient

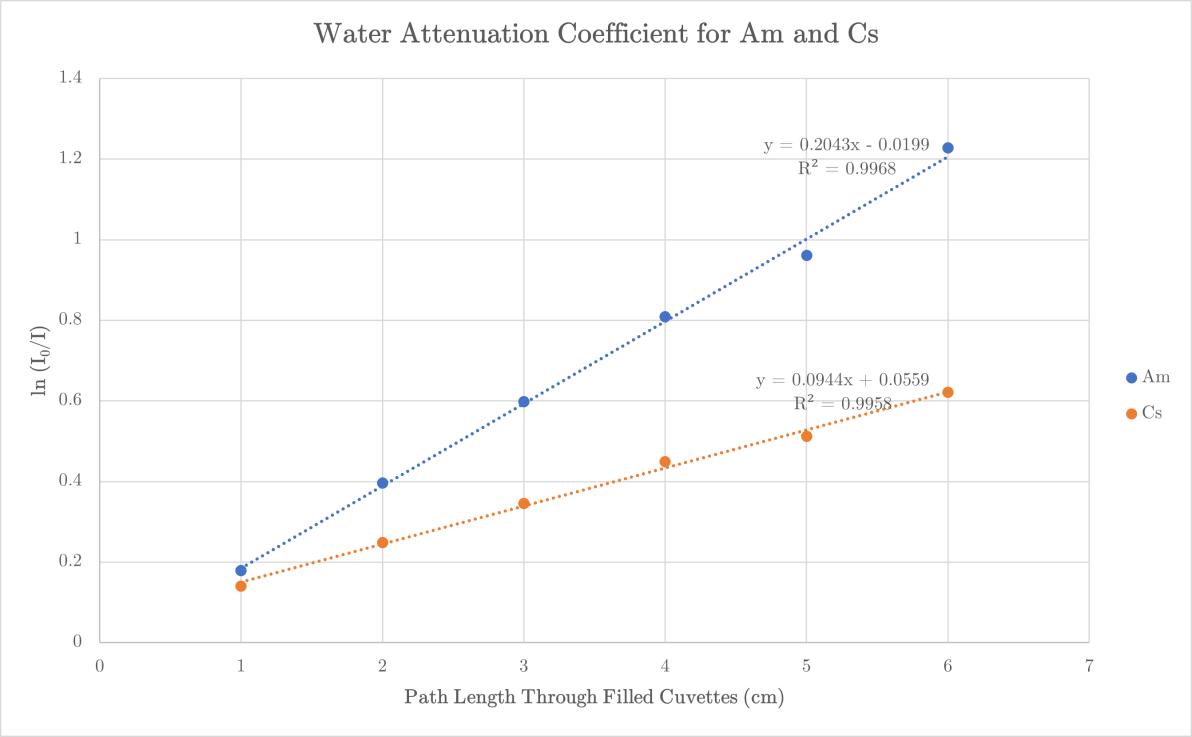


Figure B.2.: Path length through water filled cuvettes vs the corrected ln ($I_0$/I) of water. The water attenuation coefficient is the absolute value of the slope.

### B.2.2. Soil Attenuation Coefficient

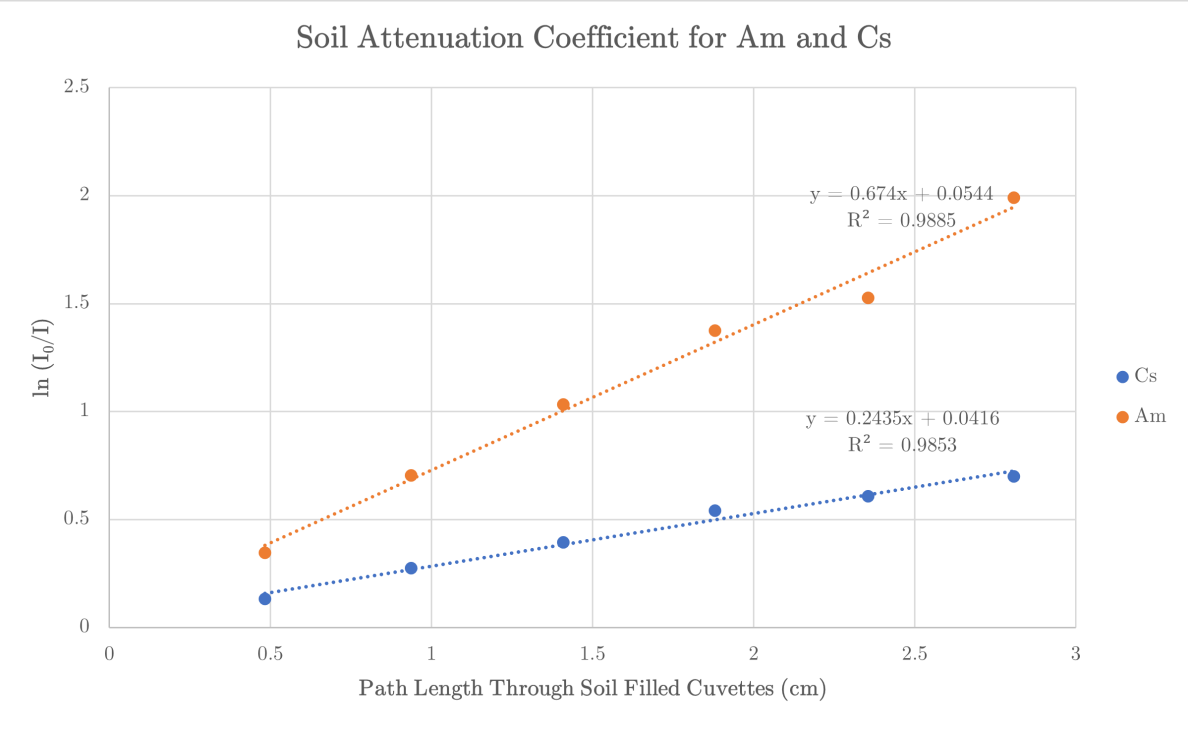


Figure B.3.: Path length through soil filled cuvettes vs the corrected ln ($I_0$/I) of soil. The soil attenuation coefficient is the absolute value of the slope.

# C. ECb Data

## C.1. Depth -5cm

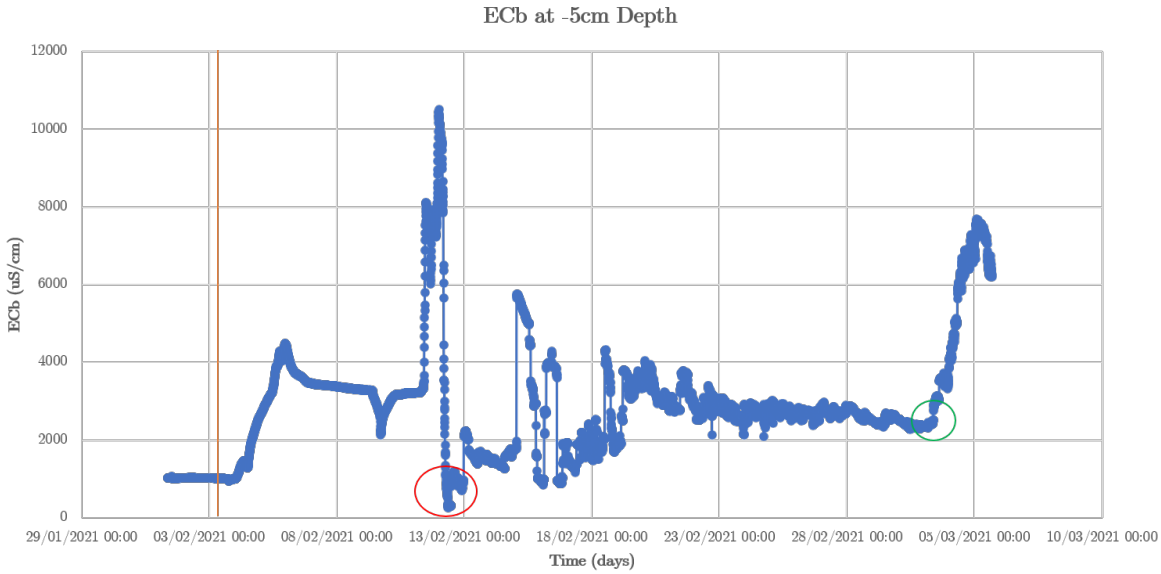


Figure C.1.: ECb at depth -5cm: Orange line illustrates when the nutrients were first injected. From 03/02 until 09/02, the ECb increases when the nutrients reaches depth -5cm and then slightly decreases when water started dripping. The same pattern can be seen to an extent from 09/02 until 12/02. Suddenly there was a significant decline in ECb on 12/02 (red circle) that it even went below the average ECb before the start of the first nutrient dripping. From then onwards, it gradually increases in a fluctuating manner, then stayed constant and increased again from 03/03 (green circle).

## C.2. Depth -20cm

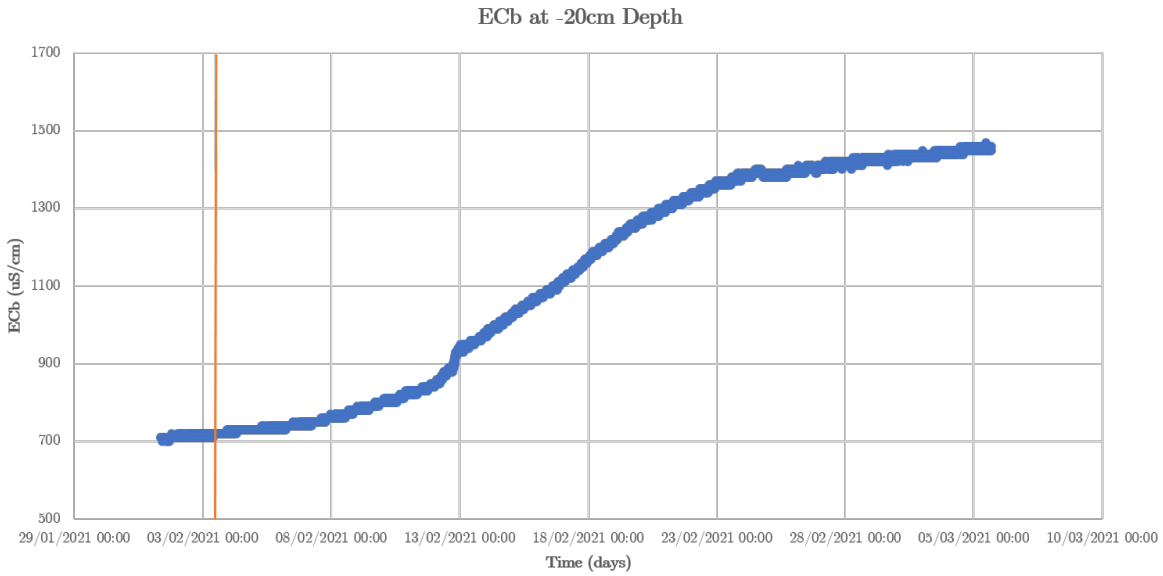


Figure C.2.: ECb at depth -20cm: Orange line illustrates when the nutrients were first injected. No notable changes in the ECb data at depth -20cm, other than that it increases due to the presence of nutrients.

# C.3. Depth -35cm

## C.3.1. Nutrient Presence

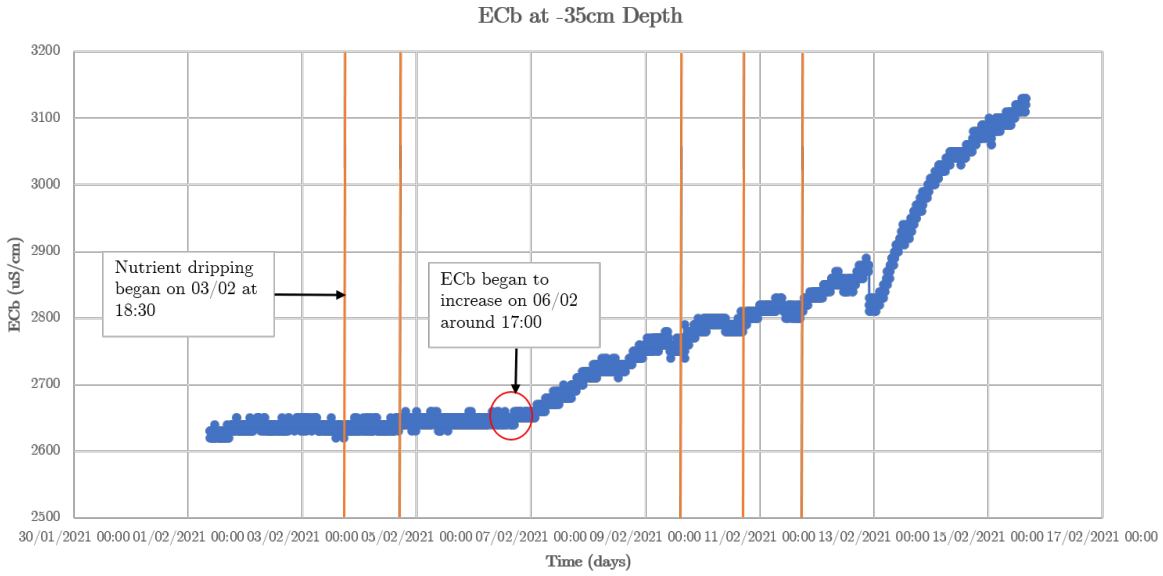


Figure C.3.: Nutrient presence at depth -35cm: The ECb data from the 5TE sensors can tell us when nutrients have reached a certain depth. Orange lines represent when the nutrients were injected. From 01/02 until 05/02 the ECb stayed relatively constant, then there was an increase from 06/02 onward. The time that it took for the nutrients to reach depth 35 cm is 70.5 hours. The velocity at which the nutrients were travelling is around 35cm/70.5hrs = 0.497 cm/hr. For comparison, the water velocity is 3.18 cm/hr. The nutrient velocity is about 15.62% of the water velocity. The retardation factor, R, can be calculated as 3.18/0.497 = 6.4. The adsorption coefficient, $K_d$, can then be computed from $K_d$ = [(R-1)*porosity]/bulk density = [(6.4-1)*0.45]/(1.61 g/cm$^3$) = 1.51 cm$^3$/g. This could explain why the nutrients took longer to travel the same distance.

### C.3.2. Overall ECb

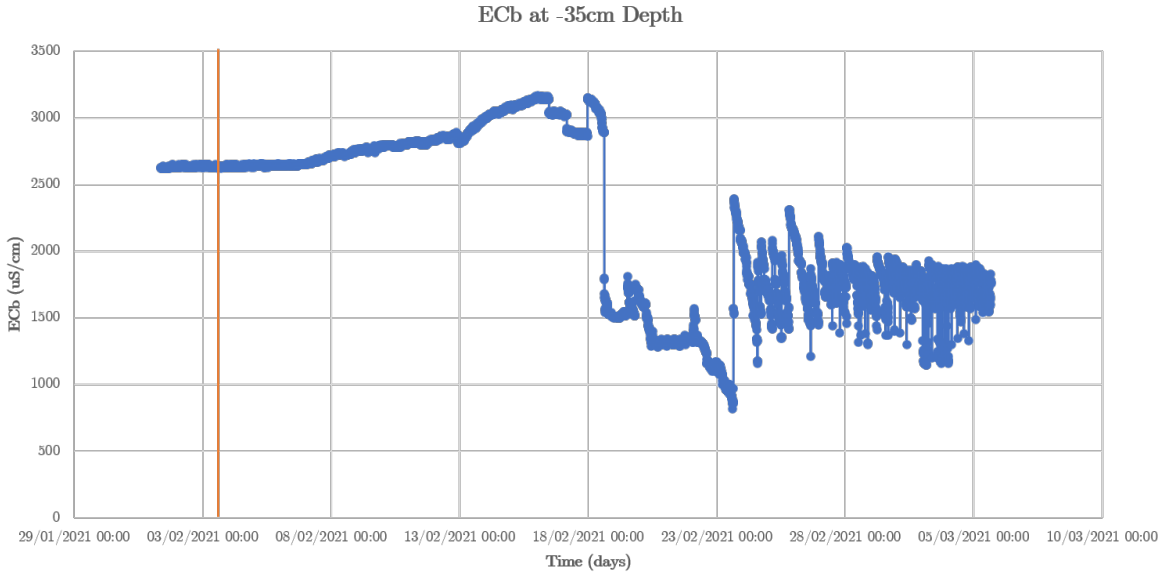


Figure C.4.: ECb at depth -35cm: Orange lines illustrated when the nutrients were injected. On 18/02, there was a sudden drop in ECb where it dropped below the starting value and then the ECb continued to decrease and suddenly increased on 23/02 and remained constant.

## C.4. Depth -46.5cm

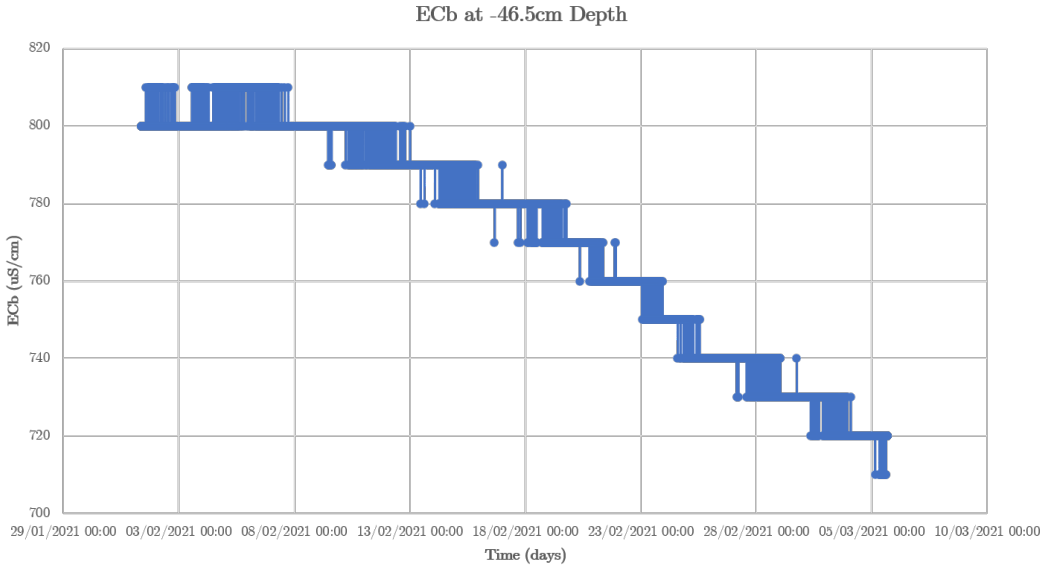


Figure C.5.: ECb at depth -46.5cm: The ECb decreases slowly over time